Am J Cancer Res 2021;11(4):1480-1502
www.ajcr.us /ISSN:2156-6976/ajcr0120269

Original Article

The PVT1/miR-612/CENP-H/CDK1 axis promotes malignant progression of advanced endometrial cancer

Rong Cong, Fanfei Kong, Jian Ma, Qing Li, Hui Yang, Xiaoxin Ma

Department of Obstetrics and Gynecology, Shengjing Hospital of China Medical University, Sanhao Street, Shenyang, People's Republic of China

Received August 13, 2020; Accepted February 24, 2021; Epub April 15, 2021; Published April 30, 2021

Abstract: Our previous study introduced the oncogenic role of the long non-coding RNA plasmacytoma variant translocation 1 (PVT1) in endometrial cancer (EC). In this study, we aimed to construct a PVT1-centered competing endogenous RNA (ceRNA) network to outline a regulatory axis that might promote the malignant progression of advanced EC. Raw Uterine Corpus Endometrial Carcinoma (UCEC) datasets were collected from The Cancer Genome Atlas (TCGA) database and used for construction of the PVT1-centered ceRNA network. The ceRNA binding sites were established using dual-luciferase assays. FISH assays displayed the co-location of PVT1 and miR-612 in EC cells. Immunohistochemistry, in situ hybridization, qRT-PCR, and western blots were used to assess the expression of miR-612 and CENP-H in EC tissues, and their functions on biological behaviours were examined by a series of *in vitro* and *in vivo* assays. Molecule interactions were illustrated by co-transfection assays. The bioinformatics analysis showed that PVT1/miR-612/CENP-H/CDK1 axis played a vital role in the malignant progression of advanced EC. MiR-612 was downregulated in EC tissues and acted as a tumour suppressor to inhibit cell proliferation, migration, invasion, and promote cell apoptosis. CENP-H was found overexpressed in EC tissues, and the expression level was correlated to diagnosis and prognosis of EC. Hyperactivated CENP-H promoted cell proliferation, migration, invasion, and inhibited cell apoptosis. Overexpressed CENP-H prevented the anti-tumour effects observed with upregulated miR-612; knockdown of miR-612 also suppressed the anti-tumour effects of downregulated PVT1. Knockdown of PVT1 together with upregulated miR-612 exerted the strongest anti-tumour effects in nude mice. These effects were mediated by CDK1 through modulation of the Akt/mTOR signaling pathway. In conclusion, the PVT1/miR-612/CENP-H/CDK1 axis promoted the malignant progression of advanced EC and could serve as a promising target for potential treatments.

Keywords: lncRNA, PVT1, endometrial cancer, miR-612, CENP-H, ceRNA, CDK1

Introduction

In developed countries, endometrial cancer (EC) is the most common gynecological cancer and the second most common cause of death from gynecological cancer [1]. EC can be classified into two groups according to its clinical stages or grades. Stage I-II ECs often have favorable outcomes with timely treatment, whereas Stage III-IV ECs typically do not respond well to surgical interventions, radiotherapy, or chemotherapy and usually have worse prognosis [2]. It's worth noticing that treatment for advanced EC is difficult because EC tumour cells have complex biological behaviours and strong resistance to existing therapeutics [3]. Therefore, there is an urgent need to determine what contributes to malignant progression of advanced EC and to analyze the underlying molecular mechanisms in order to develop more effective therapeutic strategies.

In recent years, increasing numbers of long noncoding RNA (lncRNA) have been reported to have a wide range of biological functions in regulating diverse physiological and pathological settings. Especially in tumour progression, abundant evidences have shown that lncRNAs play a pivotal role in modulating malignant behaviours of tumour cells with a series of mechanisms identified, such as epigenetic modification, transcriptional and post-transcriptional profiling [4-6]. However, most lncRNAs might function in a tissue-specific or cell type-specific manner and only a small scale of functional lncRNAs have been well characterized in

different tumours [7]. Notably, for the past two years, the plasmacytoma variant translocation 1 (PVT1) has been reported as an oncogene by a growing number of studies, including in gallbladder cancer [8], esophageal adenocarcinoma [9], breast cancer [10], gastric cancer [11], colorectal cancer [12], and so on. It is undoubted that a better understanding of the pathogenic mechanisms of PVT1 will greatly facilitate our acknowledgement on cancer development. Our previous study was the first one to introduce the oncogenic role of PVT1 in EC [13]. Recently a study by Xing [14] introduced the upstream regulator of PVT1. Combining with our achieved experience, we intend to discover how PVT1 regulates the downstream factors to promote the oncogenesis in EC.

Among the existing studies, PVT1 is usually taken as a competing endogenous RNA (ceRNA) to regulate tumour progression by interacting with miRNA and mRNA. Although Wang's review [15] systematically outlined twenty reported miRNAs interacting with PVT1 in tumour development, a mass of PVT1 targets, not limited to miRNA, remain largely unknown. Therefore, we used The Cancer Genome Atlas (TCGA) database to conduct a PVT1-centered co-expression network. Another network was performed for advanced EC to illuminate what led to the malignant progression of aggressive tumour. The networks predicted, with a high probability, that PVT1 acted as a sponge-like molecule to capture miR-612 and prevented its inhibition of Centromere protein-H (CENP-H). Moreover, CENP-H was probably associated with a cell cycle-related protein, cyclin dependent kinase 1 (CDK1), which has been shown to drive advanced EC progression by participating in the Akt signaling pathway [16]. Taken together, we speculate that PVT1/miR-612/CENP-H/CDK1 axis promotes malignant progression of advanced EC via Akt signaling pathway. As the functions of miR-612 and CENP-H haven't been reported in EC, we used two representative EC cell lines, Ishikawa and HEC-1A, to identify their roles in EC and interactions with PVT1.

Methods

Bioinformatic analysis of PVT1-centered ceRNA network

We collected raw Uterine Corpus Endometrial Carcinoma (USEC) datasets from TCGA database. Next we established a gene matrix after data processing in Perl 5.30.2 and we used R 3.6.0 software to analyze abnormally expressed lncRNAs, miRNAs, and mRNAs associated with PVT1. With the target interactions identified during this data processing, we established corresponding lncRNA-miRNA and miRNA-mRNA pairs from starBase. We then constructed a hypergeometric ceRNA network using Cytoscape 3.8.0 software, with |fold change| > 2.0 and a significance level of $P < 0.05$.

Patients and samples

A total of 57 endometrial cancer tissues and 20 normal endometrial tissues were obtained from patients who underwent hysterectomies between 2013 and 2017 in Shengjing Hospital of China Medical University. The patient informed consent is available. The clinicopathologic features of the EC patients are listed in Table S1. All specimens were evaluated by two pathologists. The patients were staged according to the International Federation of Gynecology and Obstetrics (FIGO) 2009 endometrial cancer staging system. Patients recruited in this study received no chemotherapy or radiation before surgery.

Cell lines and cell culture

The human endometrial carcinoma cell line HEC-1A and human embryonic kidney (HEK) 293T cells were acquired from the Cell Bank of the Chinese Academy of Sciences (Shanghai, China). HEC-1A and HEK 293T cells were maintained in McCoy's 5A medium (Gibco, Carlsbad, CA, USA) and high-glucose Dulbecco's Modified Eagle Medium (DMEM; Gibco), respectively. The human endometrial carcinoma cell line Ishikawa was purchased from the BeNa Culture Collection (Kunshan City, China) and grown in RPMI 1640 medium (Gibco). The culture medium was supplemented with 10% fetal bovine serum (FBS; Gibco), 50 IU/mL penicillin, and 50 mg/mL streptomycin (Invitrogen, Carlsbad, CA, USA). Cells were incubated at 37°C in a humidified incubator in the presence of 5% CO_2.

Transfection of cells

Overexpression plasmids (pcDNA3.1-PVT1, pEX4-CENP-H, pcDNA3.1-CDK1), knockdown plasmids (si-CENP-H, si-CDK1), and their respective negative control (NC) counterparts

were purchased from GenePharma (Shanghai, China). The lentivirus low-expression plasmids harboring PVT1 (LV-PVT1-RNAi 47488-1) and negative control lentivirus (hU6-MCS Ubiquitin-EGFP-IRES-puromycin) were purchased from GenePharma (Shanghai, China) and were transfected at an MOI of 50. AgomiR-612, antagomiR-612, and the respective NC were purchased from GenePharma (Shanghai, China). The Lipofectamine 3000 kit (Invitrogen, USA) was used to transfect cells with miRNAs and plasmids according to the manufacturer's instructions. The sequences of the shRNA clone, the agomiR, and the antagomiR are listed in Table S2.

RNA extraction and qRT-PCR

Total RNA was prepared using Trizol reagent (TaKaRa, Dalian, China) according to the manufacturer's instructions. Complementary DNA was synthesized with gene-specific primers or random primers using the PrimeScript RT Reagent Kit with gDNA Eraser (Takara, Dalian, China) or with the Mir-X miRNA First Strand Synthesis Kit (Takara, Dalian, China). qRT-PCR assays were performed in triplicate using the SYBR Premix Ex Taq Kit (Takara, Dalian, China) on an ABI Prism 7500 Fast Real-Time PCR System (Applied Biosystems, StepOnePlus, USA). Data for miR-612 was normalized to U6-snRNA and data for mRNA was normalized to glyceraldehyde phosphate dehydrogenase (GAPDH). The relative expression of RNAs was calculated using the comparative 2-ΔΔCt method. All primer sequences were listed in Table S3.

Western blotting analysis

Total cells were lysed using radioimmunoprecipitation assay buffer protein extraction reagent (Beyotime, Beijing, China) that was supplemented with protease inhibitors (Beyotime, Beijing, China). The protein concentrations of the lysates were measured using a bicinchonic acid (BCA) Protein Assay Kit (Beyotime, Beijing, China). After separating by 10% SDS-PAGE gel electrophoresis, the proteins were transferred to PVDF membranes. The membranes were then incubated with primary antibodies at 4°C overnight (primary antibodies are listed in Table S4), followed by incubation with horseradish peroxidase (HRP)-conjugated goat anti-mouse secondary antibody or HRP-conjugated goat anti-rabbit secondary antibody for 1.5 h. Quantity One imaging software (Bio-Rad, CA, USA) was used to visualize protein bands.

Dual-luciferase reporter assay

A reporter vector containing a fragment of the human PVT1 and CENP-H 3'-untranslated region (3'-UTR) with the predicted hsa-miR-612 binding sites was purchased from RiboBio. PVT1-mutated type and CENP-H-mutated type reporter vectors were created by mutating two putative binding sites. HEK 293T cells were seeded in 96-wells plates at a density of 1.0×10^4 cells per well and incubated for 24 h at 37°C. Next, hsa-miR-612 mimics or a negative control were co-transfected with the wild-type (WT) or mutated-type (MUT) reporter vectors using Lipofectamine 3000 (Invitrogen, CA, USA), according to the manufacturer's instruction. At 48 h after transfection, relative luciferase activity was measured using the Dual-Luciferase Reporter Assay System (Promega, WI, USA).

Fluorescence in situ hybridization (FISH)

FISH was used to identify the subcellular localization of PVT1 and miR-612 in Ishikawa and HEC-1A cells. The cells were seeded onto the cover slides in the 6-well plates. After 24 h, the slides were fixed with 4% paraformaldehyde and treated with protease K (20 ug/ml). Then the cells were pre-hybridized with pre-hybridization solution at 37°C for 1 h and hybridized with hybridization solution containing probes (5 ng/ul, Sangon, Shanghai, China) at 37°C overnight. Afterwards, the cells were washed by SSC solution and blocked by BSA. The nucleus was then stained with DAPI for 8 min. Finally, the cells were photographed under fluorescence microscopy.

Immunohistochemistry (IHC) staining and in situ hybridization (ISH)

Paraffin sections were deparaffinized and rehydrated, and then blocked with 0.3% hydrogen peroxide. After antigen retrieval, the sections were then treated with blocking solution. Slides were then incubated with rabbit anti-CENP-H (1:400 dilution, Bioss Biotechnology Co., Ltd., Beijing, China) at 4°C overnight, and then with a biotinylated goat anti-rabbit secondary antibody (Bioss Biotechnology Co., Ltd., Beijing, China) that was labeled with streptavidin horseradish peroxidase.

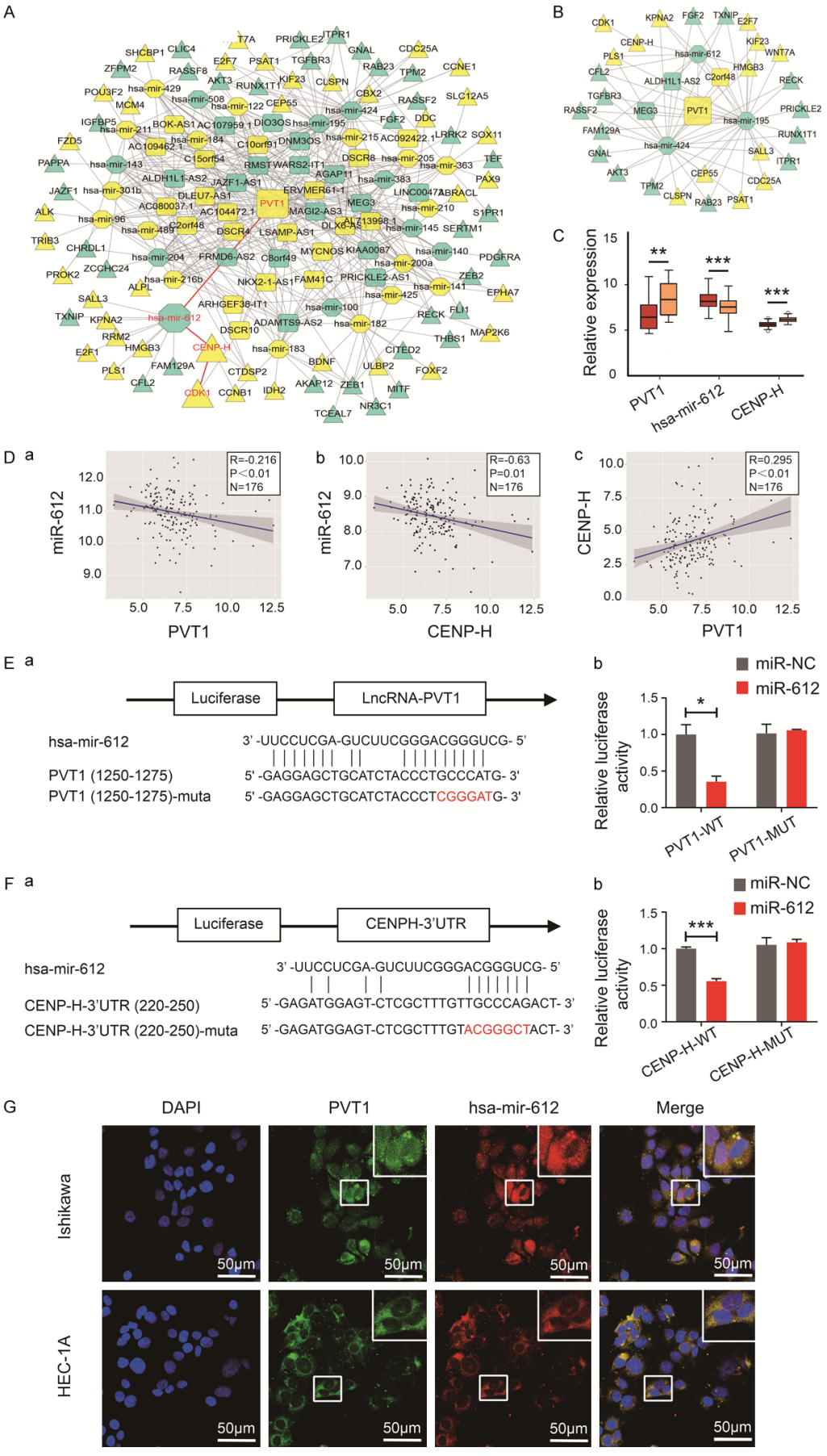
A
B
C
Relative expression
PVT1
hsa-mir-612
CENP-H
D a
R=-0.216
P<0.01
N=176
miR-612
PVT1
b
R=-0.63
P=0.01
N=176
miR-612
CENP-H
c
R=0.295
P<0.01
N=176
CENP-H
PVT1
E a
Luciferase
LncRNA-PVT1
hsa-mir-612
3' -UUCCUCGA-GUCUUCGGGACGGGUCG- 5'
PVT1 (1250-1275)
5' -GAGGAGCTGCATCTACCCTGCCCATG- 3'
PVT1 (1250-1275)-muta
5' -GAGGAGCTGCATCTACCCTCGGGATG- 3'
b
miR-NC
miR-612
Relative luciferase activity
PVT1-WT
PVT1-MUT
F a
Luciferase
CENPH-3'UTR
hsa-mir-612
3' -UUCCUCGA-GUCUUCGGGACGGGUCG- 5'
CENP-H-3'UTR (220-250)
5' -GAGATGGAGT-CTCGCTTTGTTGCCCAGACT- 3'
CENP-H-3'UTR (220-250)-muta
5' -GAGATGGAGT-CTCGCTTTGTACGGGCTACT- 3'
b
miR-NC
miR-612
Relative luciferase activity
CENP-H-WT
CENP-H-MUT
G
DAPI
PVT1
hsa-mir-612
Merge
Ishikawa
HEC-1A
50μm

Figure 1. Aberrantly activated PVT1/miR-612/CENP-H/CDK1 axis was identified. A. The PVT1-centered network based on TCGA database (|fold change| > 2.0, P < 0.05; Yellow: up-regulation, Seagreen: down-regulation; lncRNA: round rectangle, miRNA: hexagon, mRNA: triangle). B. The PVT1-centered network for Stage III-IV EC. C. Expressions of PVT1, miR-612 and CENP-H in Stage I-II EC and in Stage III-IV EC. D. The predicted relationship between PVT1 and miR-612, miR-612 and CENP-H, PVT1 and CENP-H. E. Binding targets of PVT1 and miR-612, and results of dual-luciferase assays. F. Binding targets of miR-612 and CENP-H, and results of dual-luciferase assays. G. The co-location of PVT1 and miR-612 in EC cells by FISH assays. $^{*}P < 0.05$, $^{**}P < 0.01$, $^{***}P < 0.001$ vs NC group.

For in situ hybridization, the digoxigenin-labeled oligonucleotide probe used to detect miR-612 was synthesized by Boster Biological Technology (Wuhan, China). The probe sequence was as follows: AAGGAGCTCAGAAGCCCTGCCCAGC (5'-3'). The ISH experiments were performed according to the manufacturer's instructions. All slides were visualized with diaminobenzidine (DAB) staining (Beyotime Biotechnology, Shanghai, China), and observed under a microscope.

Cell proliferation assay

Cell proliferation was measured using Cell Counting Kit-8 (CCK8, Dojindo Molecular Technologies, Kumamoto, Japan). In brief, cells at a density of 3000 cells per well were seeded in a 96-well plate. Then 10 ul CCK-8 solution was added into each well. After incubation for 4 h, the absorbance of each well at 450 nm was measured with a microplate reader (Synergy H1, BioTek, USA). For 5-ethynyl-2'-deoxyuridine (EdU) assays, EdU kit (RiboBio, Guangzhou, China) was used according to manufacturer's instructions. Twenty-four hours after transfection, EdU was dissolved into each well and incubated for 2 h. Then the cells were stained with Hoechst33342 and Apollo reagents. Images were photographed under fluorescence microscopy.

Wound healing assay

A scratch was applied to the cell monolayer using a 100-μl pipette tip. Cells were then incubated for 48 h at 37°C in complete culture medium. Images were taken 0 h and 48 h after wounding, and the distance between the wound edges was measured to assess migration ability. The original image magnification was 100 ×.

Transwell invasion assay

Transwell filter inserts (8-μM pore size; Corning, NY, USA) were pre-coated with Matrigel and washed with serum-free medium. Each upper chamber contained 2×10^4 starved cells resuspended with 200 μL serum-free media, and each lower chamber was filled with media containing 10% FBS. After incubation at 37°C for 24 h, cells were washed three times. Cells were then fixed with 4% polyoxymethylene for 1 h and stained with 0.1% crystal violet for 1 h. Cells were imaged under an inverted fluorescence microscope equipped with an image acquisition system (Nikon, Japan). The original image magnification was 200 ×.

Apoptosis and cell cycle analysis

The cells were collected after 48 h of transfection and resuspended in 1 × binding buffer. Cells were then washed and stained with Annexin V-Allophycocyanin/7-amino-actinomycin D (APC/7AAD; KeyGen Biotech, Nanjing, China) according to the manufacturer's instructions. Immediately after staining, cells were analyzed by flow cytometry (BD FACSCalibur, NJ, USA). Cells were harvested, washed, fixed with 75% ethanol at 4°C overnight, and then incubated with RNaseA and PI at 4°C for 30 min. The cell cycle was immediately detected by flow cytometry (BD FACSCalibur).

Tumour xenograft and tail vein injection experiments

Five-week-old female BALB/c athymic nude mice were maintained under specific pathogen-free conditions. Tumours were established after injection of 10^6 cells resuspended in 0.2 ml PBS into the left axilla of the mice. Xenografts were examined every 4 days with digital calipers, and tumour volume was calculated according to the following equation: tumour volume (mm^3) = (length × $width^2$)/2. Mice were sacrificed 28 days after cell injection. Samples were fixed at 4°C in paraformaldehyde and were then embedded in paraffin. All animal experiments were approved by the Scientific Research and New Technology Ethical Committee of the Shengjing Hospital of China Medical University.

Statistical analysis

All experiments were performed in triplicate. The data were presented as the mean ± standard error of the mean (SEM). Statistical analyses were performed using IBM SPSS 19.0 software (SPSS, Inc., Chicago, Illinois, USA), GraphPad Prism 8.0 software, and R 3.6.0 software (http://www.Rproject.org). A survival analysis was performed using Kaplan-Meier analysis. Hazard ratios and 95% confidence intervals (CI) were identified using the Cox proportional hazards model. Student's t-tests and one-way analysis of variance (ANOVA) tests were to compare differences. Associations between variables were analyzed using the Mann-Whitney U test or the chi-square test. Co-expressed relationships between genes were computed using the Pearson test, and were included if the absolute value of the Pearson coefficient was > 0.2. All tests were two-sided, and $P < 0.05$ was used to indicate statistical significance.

Result

Aberrantly expressed PVT1/miR-612/CENP-H/CDK1 axis was identified

The PVT1-centered ceRNA network is displayed in **Figure 1A**. Yellow represents positive correlation to PVT1, while sea green indicates negative correlation. To discover the risk factors in advanced EC, we then collected the data from Stage III-IV EC patients and generated another network in **Figure 1B**. The PVT1/miR-612/CENP-H/CDK1 axis was shown in both figures, indicating the axis played a hub role in the PVT1-centered ceRNA network, and might contribute to the aggressive progression of EC. Comparisons of the expression of PVT1, miR-612, and CENP-H in Stage I-II versus Stage III-IV EC were displayed in **Figure 1C**. The expression of PVT1 and CENP-H was significantly higher in Stage III-IV than in Stage I-II, whereas the expression of miR-612 was relatively lower in Stage III-IV than in Stage I-II. We also analyzed the relationship between the expression of PVT1, miR-612, and CENP-H. **Figure 1Da**, **1Db** demonstrates a negative association between miR-612 and PVT1 expression, and also between miR-612 and CENP-H expression. In contrast, **Figure 1Dc** shows a positive association between PVT1 and CENP-H expression.

Next, we predicted potential miR-612 binding sites in PVT1 and CENP-H, and then constructed dual-luciferase reporter plasmids (**Figure 1Ea**, **1Fa**). Dual-luciferase reporter assays (**Figure 1Eb**, **1Fb**) showed that the luciferase activities of PVT1-WT and CENP-H-WT were remarkably repressed by miR-612 mimics compared with pre-miR-NC. However, the luciferase activities of PVT1-MUT and CENP-H-MUT exhibited no significant changes regardless of co-transfection with miR-612 mimic or pre-miR-NC. The FISH assay demonstrated that PVT1 and miR-612 were principally co-localized in the cytoplasm of EC cells (**Figure 1G**). These results imply that PVT1 may act as a sponge to capture miR-612 and competitively interfere with its binding to CENP-H.

miR-612 is poorly expressed in EC tissues and acts as a tumour suppressor

In our previous study, we reported that PVT1 was overexpressed in EC tissues [13]. Data from TCGA showed that a higher level of PVT1 in EC patients was significantly associated with a poorer survival (Figure S1A). Expression of the putative PVT1 target, miR-612, was first assessed by ISH and qRT-PCR assays. **Figure 2A**, **2B** shows a dramatic decrease in the expression of miR-612 in EC tissues, and expression level continuously declines with increasing malignant progression. Patient prognosis was described by Kaplan-Meier analysis, which showed that low miR-612 level was associated with poor outcome (**Figure 2Bb**).

To confirm the potential effects of miR-612 on EC cells, both Ishikawa and HEC-1A cell lines were transfected with agomiR-612 or antagomiR-612. PCR results showed that transfection with agomiR-612 significantly increased miR-612 expression, whereas transfection with antagomiR-612 significantly reduced miR-612 expression (Figure S2A). Cell counting kit-8 (CCK-8) and 5-Ethynyl-2'-deoxyuridine (EdU) assays showed that proliferation was inhibited in both cell lines after transfection with agomiR-612, but proliferation was increased in cells after transfection with antagomiR-612 (**Figure 2C**, **2D**). Migration and invasion ability of tumour cells was reduced in response to miR-612 overexpression, but was increased upon knockdown of miR-612 expression (**Figure 2E**, **2F**). Flow cytometry assays showed

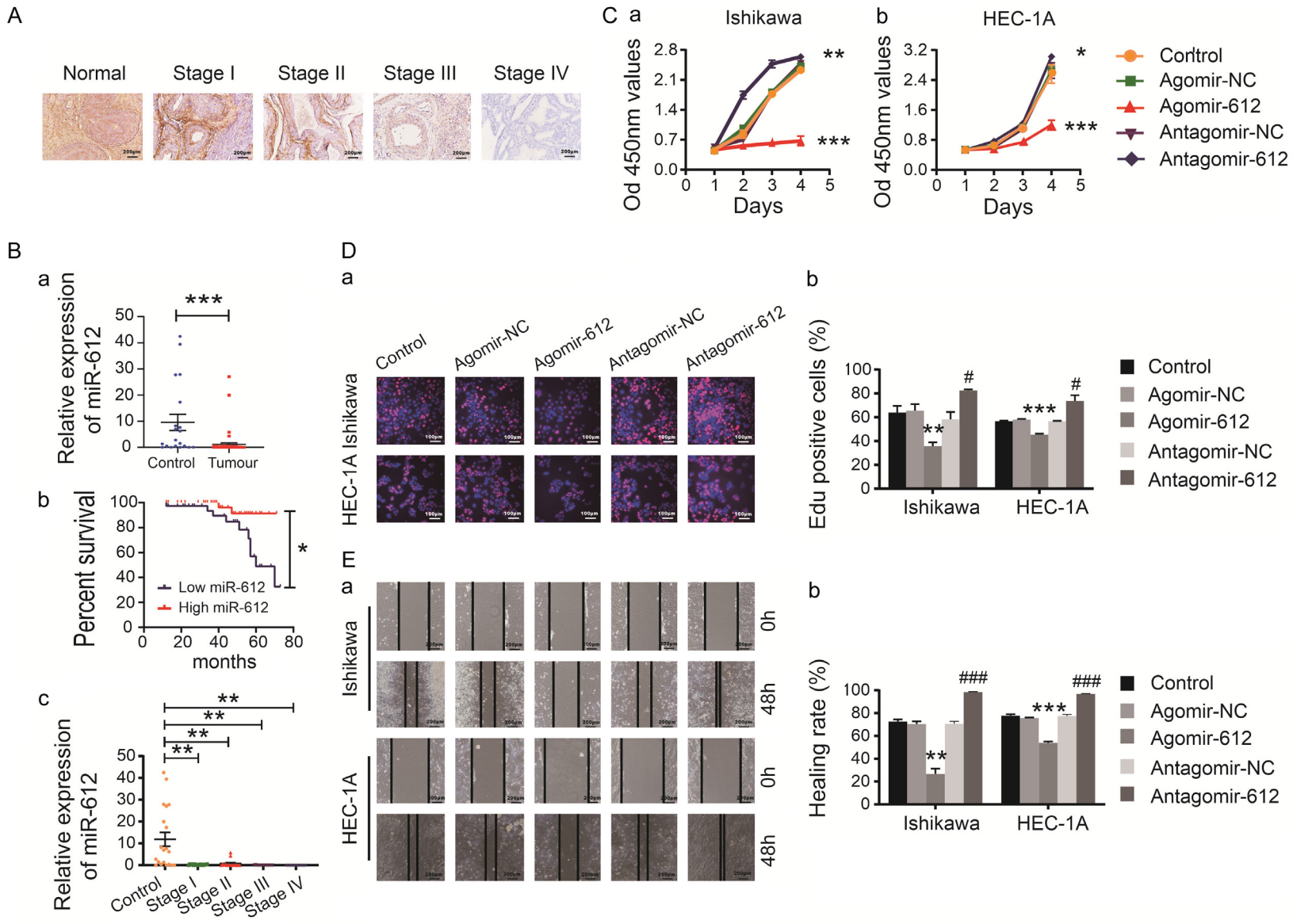
A
Normal
Stage I
Stage II
Stage III
Stage IV
C a
Ishikawa
Od 450nm values
Days
b
HEC-1A
Control
Agomir-NC
Agomir-612
Antagomir-NC
Antagomir-612
B
a
Relative expression of miR-612
Control
Tumour
b
Percent survival
Low miR-612
High miR-612
months
c
Relative expression of miR-612
Control
Stage I
Stage II
Stage III
Stage IV
D
a
Control
Agomir-NC
Agomir-612
Antagomir-NC
Antagomir-612
HEC-1A Ishikawa
b
Edu positive cells (%)
Ishikawa
HEC-1A
E
a
Ishikawa
HEC-1A
0h
48h
b
Healing rate (%)

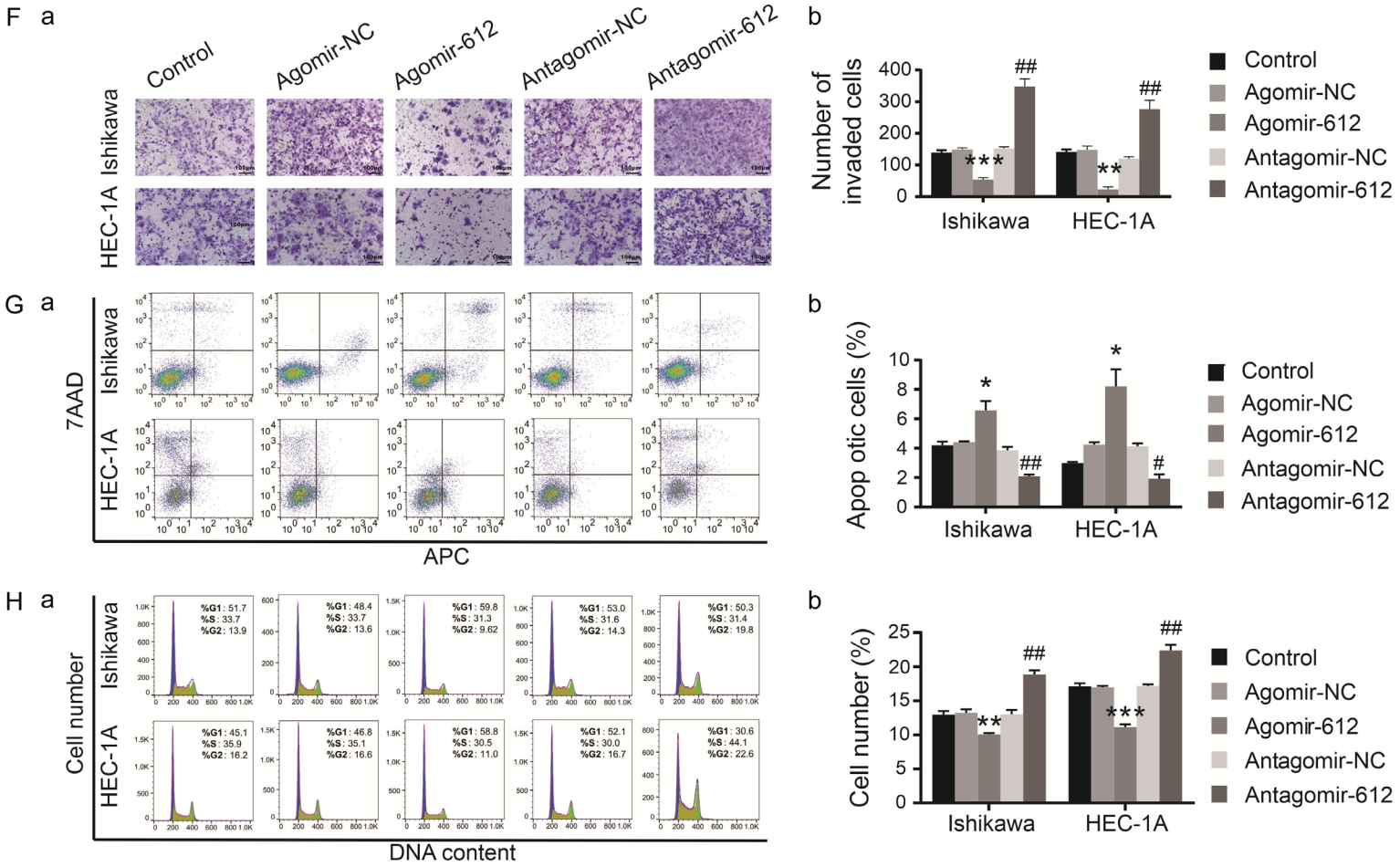

Figure 2. miR-612 is poorly expressed in EC tissues and acts as a tumour suppressor. A and B. Expression of miR-612 in different stages EC tissues and normal tissues, and its relationship to prognosis. C. Effects of miR-612 on cell proliferation in Ishikawa and HEC-1A evaluated by CCK-8 assays. D. Effects of miR-612 on cell proliferation in Ishikawa and HEC-1A evaluated by EdU assays. E. Effects of miR-612 on cell migration in Ishikawa and HEC-1A evaluated by wound healing assays. F. Effects of miR-612 on cell invasion in Ishikawa and HEC-1A evaluated by Transwell assays. G. Effects of miR-612 on cell apoptosis in Ishikawa and HEC-1A evaluated by flow cytometry. H. Effects of miR-612 on cell cycle in Ishikawa and HEC-1A evaluated by flow cytometry. Data are presented as the mean ± SEM (n = 3 per group). $^{*}P < 0.05$, $^{**}P < 0.01$, $^{***}P < 0.001$ vs agomir-NC group, $^{\#}P < 0.05$, $^{\#\#}P < 0.01$, $^{\#\#\#}P < 0.001$ vs antagomir-NC group.

that upregulation of miR-612 expression notably enhanced cell apoptosis (**Figure 2G**) and reduced the proportion of cells at G2-M phase (**Figure 2H**). In contrast, opposite trends were observed after knockdown of miR-612.

CENP-H is overexpressed in EC tissues and functions as an oncogene

IHC assays showed an abnormal level of CENP-H expression in EC, and this was positively correlated with increasing stages of EC (**Figure 3A**). Similarly, western blot assays showed that CENP-H protein expression was significantly higher in EC tissues than in normal endometrial tissues, and the expressions were correlated with survival time and clinical stages of EC (**Figure 3B**). qRT-PCR assays revealed that CENP-H expression was also increased in EC compared to normal tissues (Figure S1B). The trends of mRNA expression levels were consistent with those of protein levels in clinical prognosis and stages (Figure S1C, S1D). Additionally, CENP-H expressions were negatively correlated with miR-612 expressions in the tissues (Figure S1E, $R^2 = 0.11$, $P = 0.0035$). Receiver operating characteristic curves (ROC) were performed to evaluate the clinical value of CENP-H (Figure S1F, S1G). The area under curve (AUC) was 0.796 (95% CI = 0.655-0.936, $P < 0.001$) for diagnostic ROC and was 0.783 (95% CI = 0.657-0.908, $P = 0.002$) for prognostic ROC, indicating that CENP-H could be a novel diagnostic and prognostic indicator of EC.

We next studied the role of CENP-H in regulating the biological behaviour of tumour cells. A qRT-PCR assay showed that transfection with pEX4-CENP-H significantly increased CENP-H expression in both cell lines, whereas transfection with si-CENP-H decreased CENP-H expression (Figure S2B). Further analysis showed that knockdown of CENP-H inhibited proliferation, migration, and invasion of both cell lines, whereas overexpression of CENP-H promoted cell proliferation, migration, and invasion (**Figure 3C-F**). Additionally, knockdown of CENP-H enhancen cell apoptosis and the proportion of cells at G2-M phase decreased (**Figure 3G**, **3H**). In contrast, overexpression of CENP-H reduced cell apoptosis and more cells were found at G2-M phase. Taken together, these data suggest that CENP-H expression is correlated with poor outcomes in EC.

The anti-tumour effects of miR-612 are mediated by CENP-H

The network in **Figure 1** demonstrates the negative correlation between miR-612 and CENP-H expression. We transfected agomiR-612 or antagomiR-612 into the two cell lines for verification. As expected, the expression of CENP-H decreased when miR-612 was overexpressed, and the expression of CENP-H significantly increased when miR-612 was downregulated (**Figure 4A**). To elucidate whether the anti-tumour effects of miR-612 overexpression could be blocked with CENP-H overexpression, both cell lines were transfected with agomiR-612 or pEX4-CENP-H and divided into four groups: control, miR-612(+)-NC, miR-612(+), and miR-612(+)+CENP-H(+). When cells were co-transfected with pEX4-CENP-H and agomiR-612, cell proliferation, migration, and invasion were attenuated compared to the miR-612(+) group (**Figure 4B-E**). In the co-transfection group, there was also a reduction in apoptosis and an increase in the number of cells at G2-M phase (**Figure 4F**, **4G**). Therefore, these data support that CENP-H is a functional target of miR-612 and it mediates the anti-tumour effects of miR-612.

The anti-tumour effects of PVT1 downregulation are mediated by miR-612 and CENP-H

To confirm the regulatory effects of PVT1 on miR-612 and CENP-H, we transfected pcDNA3.1-PVT1 or LV-PVT1-RNAi into both cell lines. In the PVT1 knockdown group, miR-612 expression was significantly increased while CENP-H expression was significantly decreased, and vice versa (**Figure 5A**, **5B**). In order to determine how downregulation of PVT1 expression conferred anti-tumour effects, both PVT1 and miR-612 were downregulated in Ishikawa and HEC-1A cell lines. The cells were divided into four groups: control, PVT1(-)-NC, PVT1(-), and PVT1(-)+miR-612(-). Cells with downregulated PVT1 expression exhibited strong anti-tumour behaviours, including increased cell proliferation, migration, and invasion abilities, and enhancement of cell apoptosis (**Figure 5C-H**). By contrast, these anti-tumour effects were lost where both PVT1 and miR-612 were downregulated. Moreover, CENP-H expression was decreased in the PVT1(-) group, but was recovered in the PVT1(-)+miR-612(-) group (**Figure 5B**). Thus, the PVT1/miR-612/CENP-H

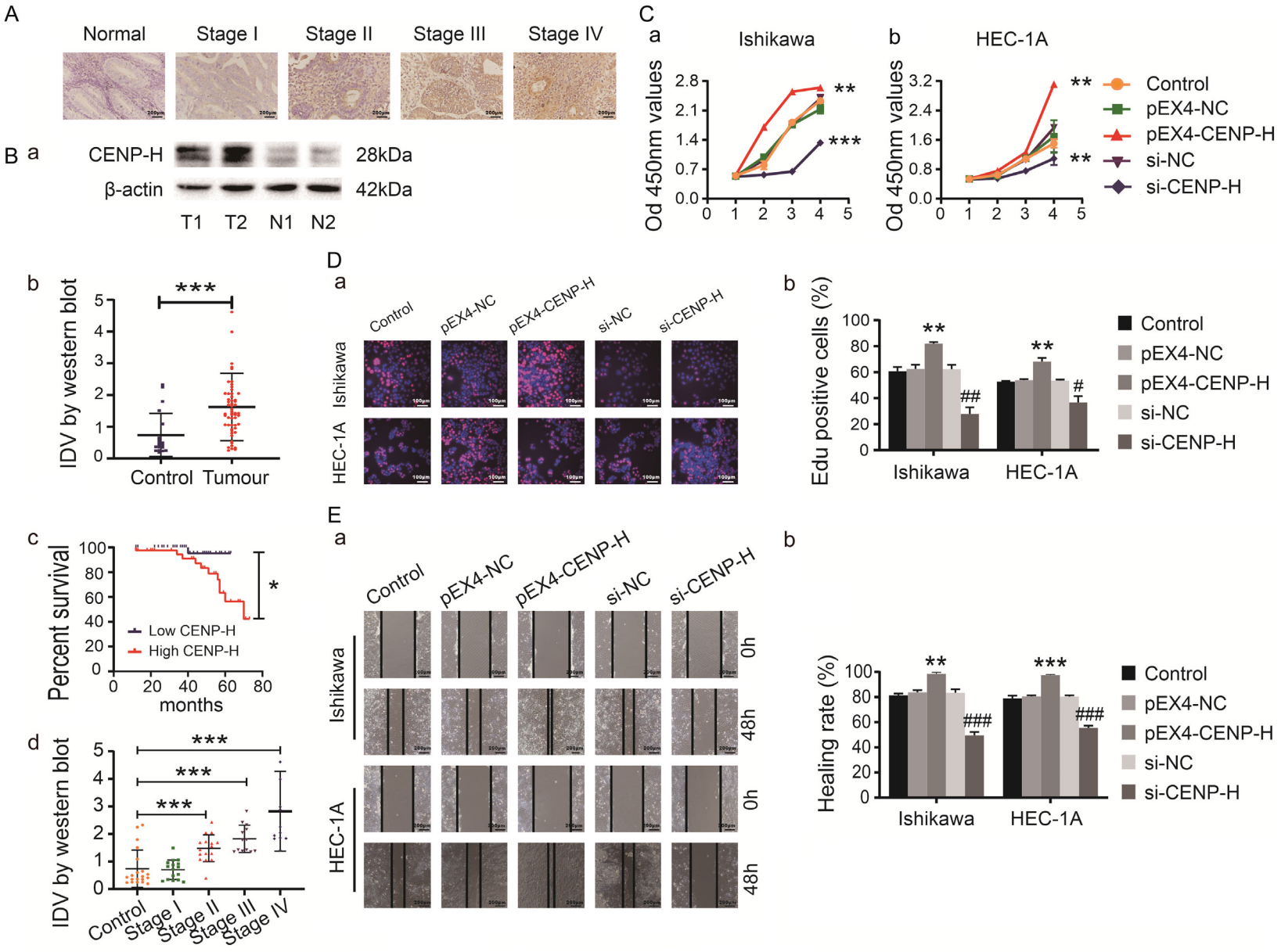
A
Normal
Stage I
Stage II
Stage III
Stage IV
B a
CENP-H
β-actin
28kDa
42kDa
T1 T2 N1 N2
b
IDV by western blot
***
Control Tumour
c
Percent survival
Low CENP-H
High CENP-H
months
*
d
IDV by western blot
***
Control
Stage I
Stage II
Stage III
Stage IV
C
a
Ishikawa
Od 450nm values
**
***
b
HEC-1A
Od 450nm values
**
**
Control
pEX4-NC
pEX4-CENP-H
si-NC
si-CENP-H
D
a
Control
pEX4-NC
pEX4-CENP-H
si-NC
si-CENP-H
Ishikawa
HEC-1A
b
Edu positive cells (%)
**
**
##
#
Ishikawa
HEC-1A
Control
pEX4-NC
pEX4-CENP-H
si-NC
si-CENP-H
E
a
Control
pEX4-NC
pEX4-CENP-H
si-NC
si-CENP-H
Ishikawa
HEC-1A
0h
48h
0h
48h
b
Healing rate (%)
**
***
###
###
Ishikawa
HEC-1A
Control
pEX4-NC
pEX4-CENP-H
si-NC
si-CENP-H

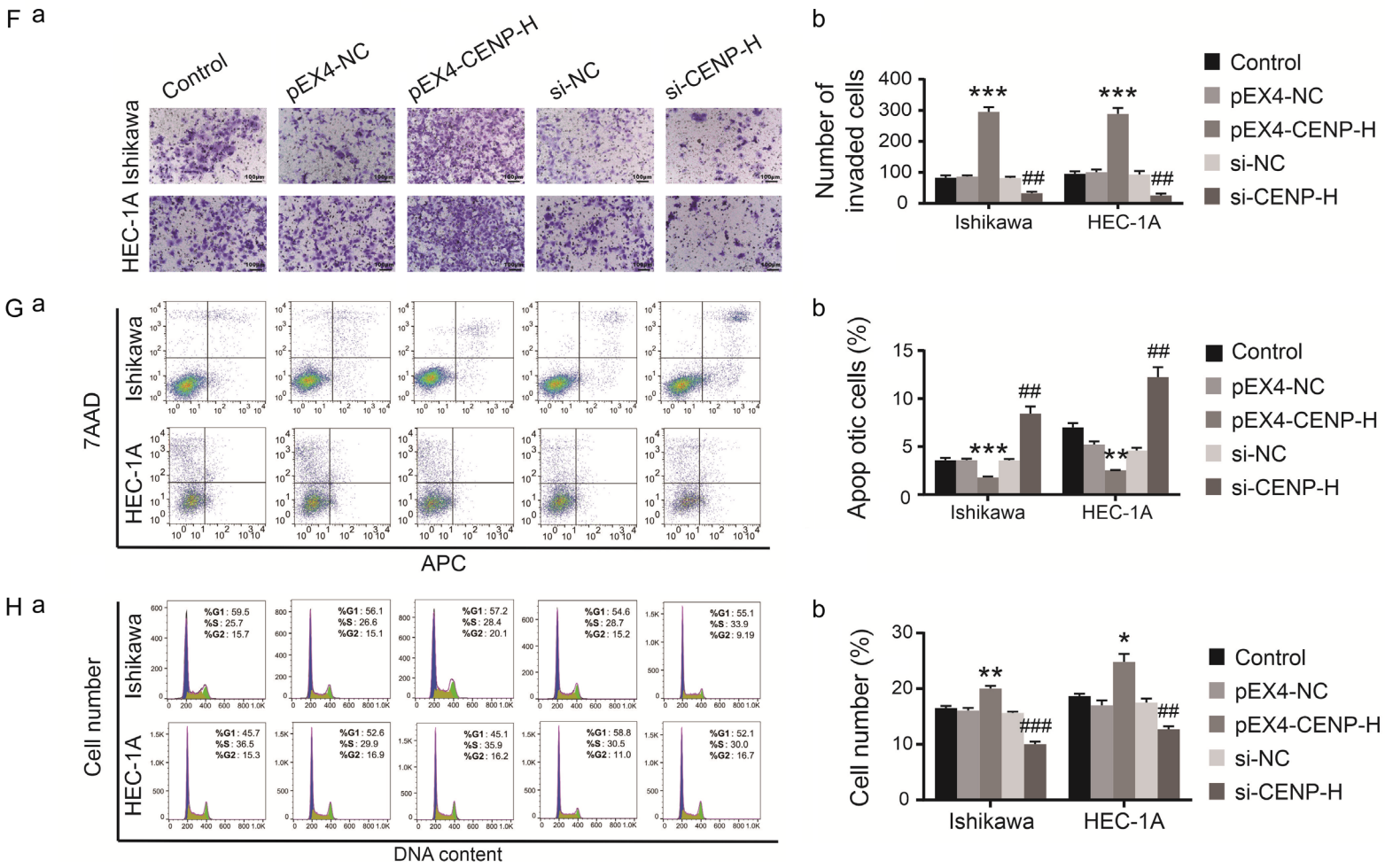

Figure 3. CENP-H is overexpressed in EC tissues and functions as an oncogene. A and B. Expression of CENP-H in different stages EC tissues and normal tissues, and its relationship to prognosis. C. Effects of CENP-H on cell proliferation in Ishikawa and HEC-1A evaluated by CCK-8 assays. D. Effects of CENP-H on cell proliferation in Ishikawa and HEC-1A evaluated by EdU assays. E. Effects of CENP-H on cell migration in Ishikawa and HEC-1A evaluated by wound healing assays. F. Effects of CENP-H on cell invasion in Ishikawa and HEC-1A evaluated by Transwell assays. G. Effects of CENP-H on cell apoptosis in Ishikawa and HEC-1A evaluated by flow cytometry. H. Effects of CENP-H on cell cycle in Ishikawa and HEC-1A evaluated by flow cytometry. Data are presented as the mean ± SEM (n = 3 per group). $^{*}P < 0.05$, $^{**}P < 0.01$, $^{***}P < 0.001$ vs pEX4-NC group, $^{\#}P < 0.05$, $^{\#\#}P < 0.01$, $^{\#\#\#}P < 0.001$ vs si-NC group.

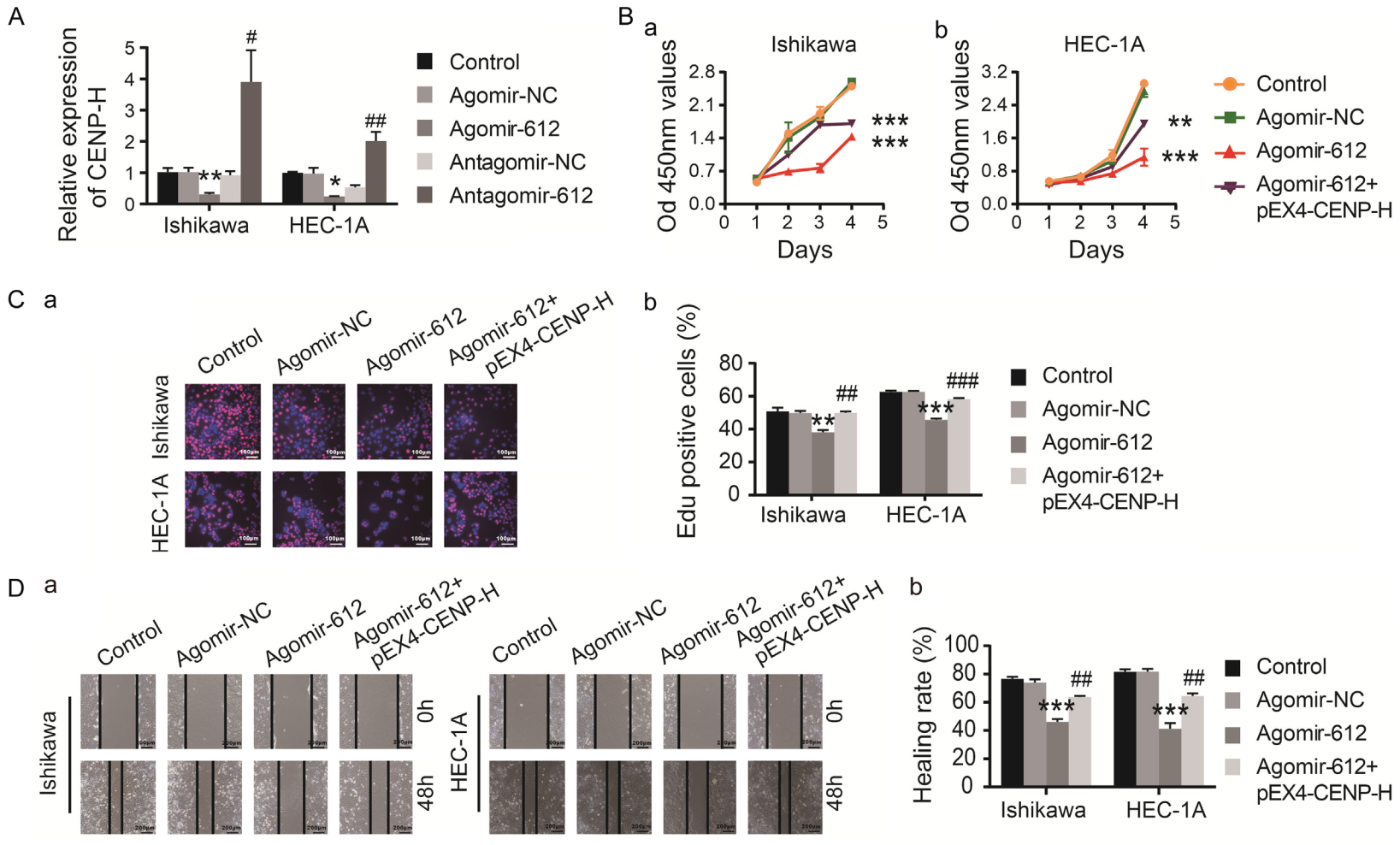
A
Relative expression of CENP-H
Ishikawa
HEC-1A
Control
Agomir-NC
Agomir-612
Antagomir-NC
Antagomir-612
B
a
Ishikawa
Od 450nm values
Days
b
HEC-1A
Od 450nm values
Days
Control
Agomir-NC
Agomir-612
Agomir-612+ pEX4-CENP-H
C
a
Control
Agomir-NC
Agomir-612
Agomir-612+ pEX4-CENP-H
Ishikawa
HEC-1A
b
Edu positive cells (%)
Ishikawa
HEC-1A
Control
Agomir-NC
Agomir-612
Agomir-612+ pEX4-CENP-H
D
a
Control
Agomir-NC
Agomir-612
Agomir-612+ pEX4-CENP-H
Ishikawa
HEC-1A
0h
48h
b
Healing rate (%)
Ishikawa
HEC-1A
Control
Agomir-NC
Agomir-612
Agomir-612+ pEX4-CENP-H

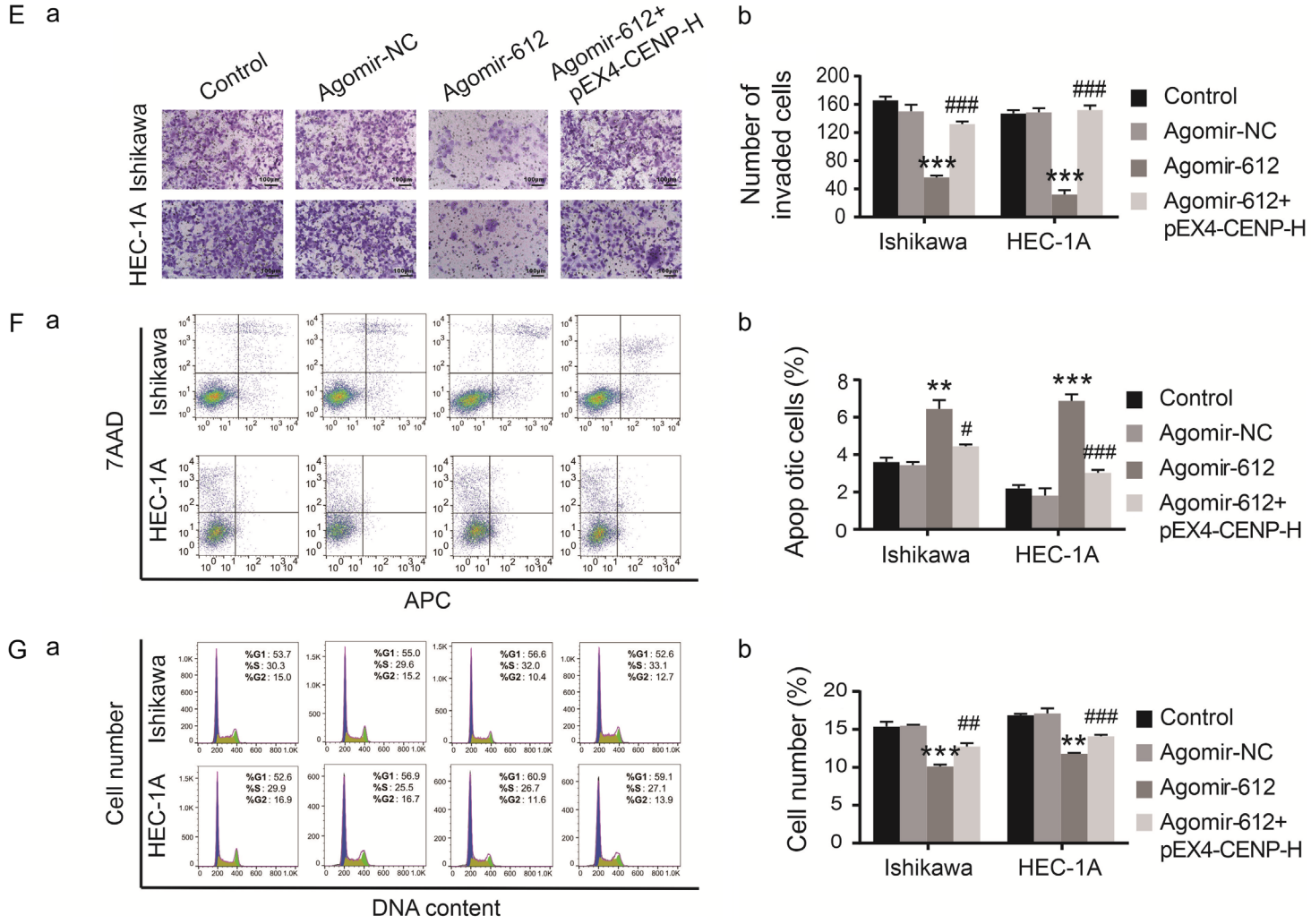

Figure 4. The anti-tumour effects of miR-612 are mediated by CENP-H. A. Expression of CENP-H after the altering miR-612 expression in Ishikawa and HEC-1A. B. Proliferation of Ishikawa and HEC-1A after co-transfection with miR-612 and CENP-H evaluated by CCK-8 assays. C. Proliferation of Ishikawa and HEC-1A after co-transfection with miR-612 and CENP-H evaluated by EdU assays. D. Migration of Ishikawa and HEC-1A after co-transfection with miR-612 and CENP-H evaluated by wound healing assays. E. Invasion of Ishikawa and HEC-1A after co-transfection with miR-612 and CENP-H evaluated by Transwell assays. F. Apoptosis of Ishikawa and HEC-1A after co-transfection with miR-612 and CENP-H evaluated by flow cytometry. G. Cell cycle of Ishikawa and HEC-1A after co-transfection with miR-612 and CENP-H evaluated by flow cytometry. Data are presented as the mean ± SEM (n = 3 per group). $^{*}P < 0.05$, $^{**}P < 0.01$, $^{***}P < 0.001$ vs agomir-NC group, $^{\#}P < 0.05$, $^{\#\#}P < 0.01$, $^{\#\#\#}P < 0.001$ vs agomir-612 group, $^{\&}P < 0.05$ vs sh-PVT1 group.

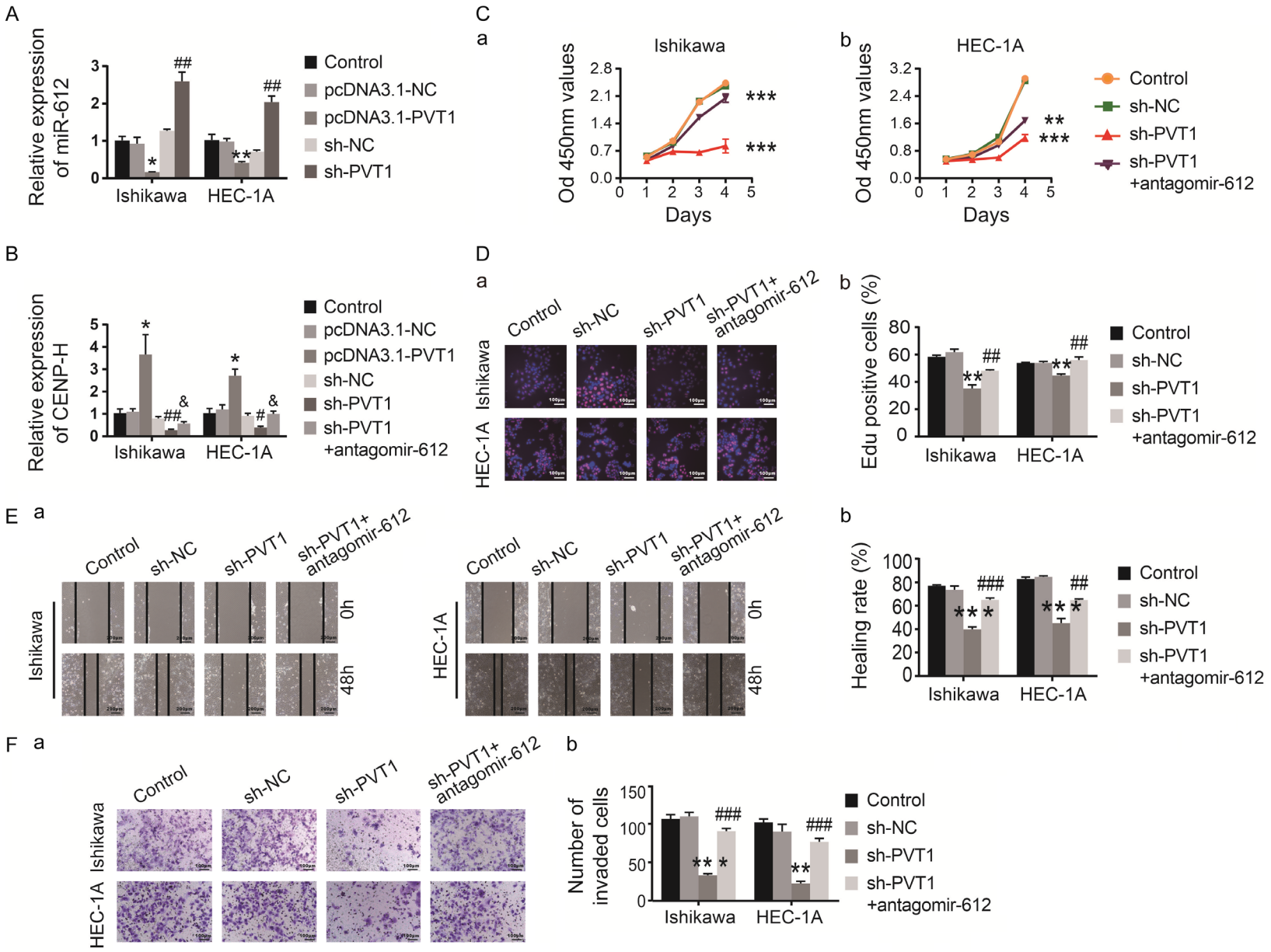
A
Relative expression of miR-612
Ishikawa
HEC-1A
Control
pcDNA3.1-NC
pcDNA3.1-PVT1
sh-NC
sh-PVT1
B
Relative expression of CENP-H
sh-PVT1 +antagomir-612
C
a
Ishikawa
Od 450nm values
Days
b
HEC-1A
D
a
Control
sh-NC
sh-PVT1
sh-PVT1+ antagomir-612
b
Edu positive cells (%)
E
a
0h
48h
b
Healing rate (%)
F
a
b
Number of invaded cells

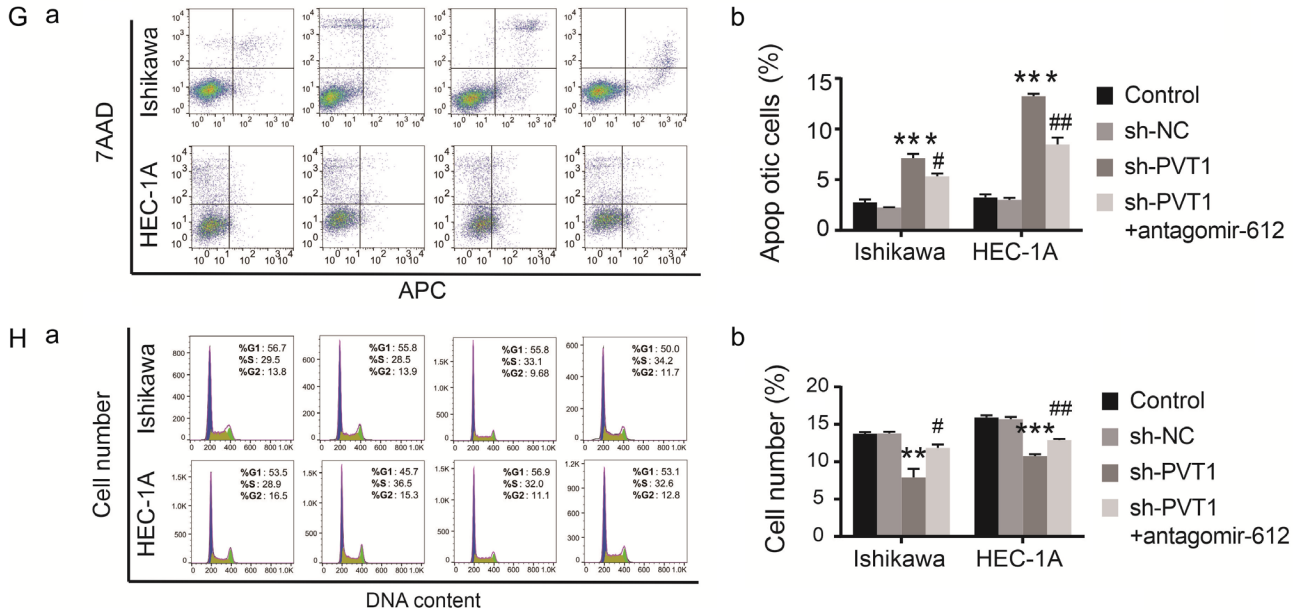

Figure 5. The anti-tumour effects of PVT1 downregulation are mediated by miR-612 and CENP-H. A. Expression of miR-612 after the altering PVT1 expression in Ishikawa and HEC-1A. B. Expression of CENP-H after the altering PVT1 expression in Ishikawa and HEC-1A. C. Proliferation of Ishikawa and HEC-1A after co-transfection with PVT1 and miR-612 evaluated by CCK-8 assays. D. Proliferation of Ishikawa and HEC-1A after co-transfection with PVT1 and miR-612 evaluated by EdU assays. E. Migration of Ishikawa and HEC-1A after co-transfection with PVT1 and miR-612 evaluated by wound healing assays. F. Invasion of Ishikawa and HEC-1A after co-transfection with PVT1 and miR-612 evaluated by Transwell assays. G. Apoptosis of Ishikawa and HEC-1A after co-transfection with PVT1 and miR-612 evaluated by flow cytometry. H. Cell cycle of Ishikawa and HEC-1A after co-transfection with PVT1 and miR-612 evaluated by flow cytometry. Data are presented as the mean ± SEM (n = 3 per group). $^{*}P < 0.05$, $^{**}P < 0.01$, $^{***}P < 0.001$ vs sh-NC group, $^{\#}P < 0.05$, $^{\#\#}P < 0.01$, $^{\#\#\#}P < 0.001$ vs sh-PVT1 group.

ceRNA network is intact and contributes to the biological behaviour of EC cells.

CDK1 mediates the connection between the PVT1/miR-612/CENP-H network and the Akt/mTOR signaling pathway

Figure 1 indicates that CDK1 expression was positively associated with PVT1 expression, as with CENP-H. Using the bioinformatic tool STRING V11.0 (https://string-db.org), we predicted that CDK1 expression was positively correlated to CENP-H expression. Moreover, one previously published article demonstrated that CDK1 positively regulated the Akt/mTOR signaling pathway [16]. Therefore, we next assessed the expression of CDK1 and activation of the Akt/mTOR signaling pathway using western blot analysis (**Figure 6A**). After upregulation of PVT1 and CENP-H as well as downregulation of miR-612, we found increased CDK1, p-Akt, and p-mTOR expression in both cell lines. In contrast, in cells with downregulated PVT1 and CENP-H, as well as upregulated miR-612, CDK1, p-Akt, and p-mTOR expression levels were decreased. With respect to the co-transfection groups, CDK1 expression was significantly higher in the miR-612(+)+CENP-H(+) and PVT1(-)+miR-612(-) groups than in miR-612(+) and PVT1(-) groups, respectively. Western blot analysis also demonstrated that the CDK1 expression was consistent with that of CENP-H. In order to determine whether CDK1 mediated the function of CENP-H, we co-transfected both cell lines with si-CENP-H and pcDNA3.1-CDK1. The results showed that overexpressed CDK1 significantly rescued Akt/mTOR signaling activity against inhibition with si-CENP-H. The transfection efficacy of pcDNA3.1-CDK1 was shown in Figure S2C. The statistical results of western blot were displayed as bar graphs in Figure S3.

Knockdown of PVT1 and overexpression of miR-612 suppressed tumour growth in an EC xenograft mouse model

Thus far, we have ascertained that knockdown of PVT1 and overexpression of miR-612 in cell lines confers anti-tumour effects. Next, we verified the functions of PVT1 and miR-612 in an EC xenograft mouse model. Mice were divided into control, sh-NC, miR-NC, and sh-PVT1+agomiR-612 groups and injected with corresponding transfected Ishikawa or HEC-1A cells. As shown in **Figure 6B**, **6C**, tumour size was smallest in the sh-PVT1+agomiR-612 group. tumour sizes were smaller in the sh-PVT1 and agomiR-612 groups than those in the control group and corresponding NC groups, but were larger than those in the combined sh-PVT1+agomiR-612 group. Similarly, IHC assays showed that CENP-H protein expression was the lowest in the combined sh-PVT1+agomiR-612 group (**Figure 6D**). These results suggest that knockdown of PVT1 combined with overexpression of miR-612 significantly suppressed EC tumour growth *in vivo*.

Discussion

EC is a malignant disease that threatens the health of women worldwide. Especially advanced EC tends to invade adjacent normal tissues and is more resistant to chemotherapy [17]. In this study, for the first time, we conducted bioinformatics analysis with TCGA database to display a PVT1-centered network, which suggested that PVT1/miR-612/CENP-H/CDK1 axis played a pivotal role in the pathogenesis of EC. Further analysis on Stage III-IV EC emphasized the role of this axis in aggressive malignancy. In addition, our findings suggest that PVT1 expression was negatively correlated with miR-612 expression, but positively correlated with expression of CENP-H and CDK1 in EC. Using dual-luciferase reporter assays, we showed that miR-612 binds to PVT1 and CENP-H. Thus, we speculate that PVT1/miR-612/CENP-H forms a ceRNA network and functions via the interaction with CENP-H and CDK1.

Accordingly, the lncRNA PVT1 has been reported as an important oncogene in various human cancers. Previous studies have revealed that PVT1 contributes to carcinogenesis via several mechanisms. Wu [18] reported that expression of lncRNA PVT1 was higher in ocular uveal melanoma tissues and suppressed miR-17-3p. This in turn caused an increase in expression of mouse double minute 2 (MDM2), which activated the p53 signaling pathway and promoted tumourigenesis. Shen [19] demonstrated that downregulation of PVT1 repressed esophageal carcinoma progression and promoted tumour cell apoptosis via increased miR-145-mediated inhibition of Fascin actin-bundling protein 1 (FSCN1). Zhao [11] introduced another mechanism, through which lncRNA PVT1 increased protein stability of phosphorylated signal trans-

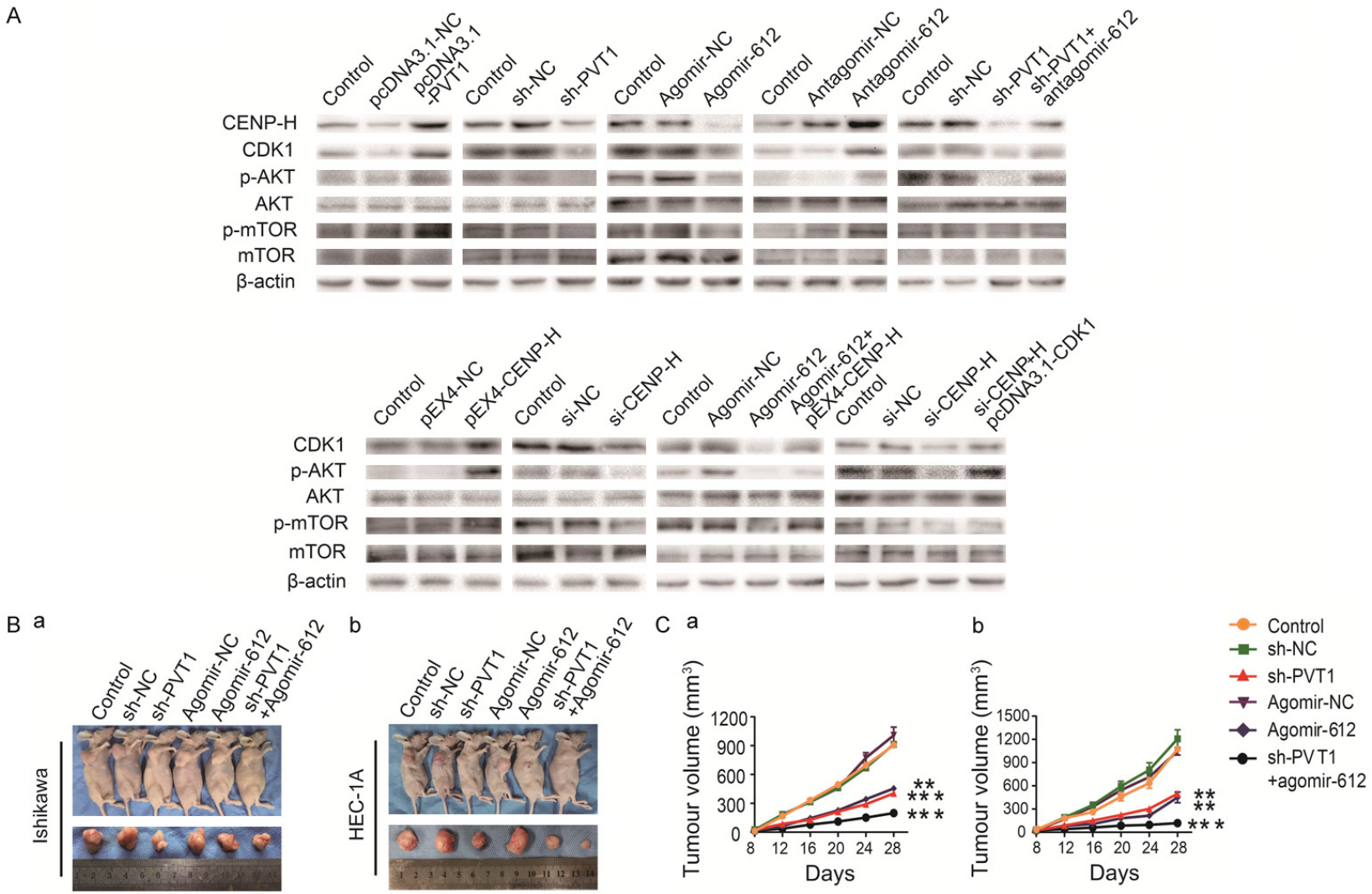
A
Control
pcDNA3.1-NC
pcDNA3.1 -PVT1
Control
sh-NC
sh-PVT1
Control
Agomir-NC
Agomir-612
Control
Antagomir-NC
Antagomir-612
Control
sh-NC
sh-PVT1
sh-PVT1+ antagomir-612
CENP-H
CDK1
p-AKT
AKT
p-mTOR
mTOR
β-actin
Control
pEX4-NC
pEX4-CENP-H
Control
si-NC
si-CENP-H
Control
Agomir-NC
Agomir-612
Agomir-612+ pEX4-CENP-H
Control
si-NC
si-CENP-H
si-CENP-H pcDNA3.1-CDK1
CDK1
p-AKT
AKT
p-mTOR
mTOR
β-actin
B a
Control
sh-NC
sh-PVT1
Agomir-NC
Agomir-612
sh-PVT1 +Agomir-612
Ishikawa
b
HEC-1A
C a
Tumour volume (mm3)
Days
b
Control
sh-NC
sh-PVT1
Agomir-NC
Agomir-612
sh-PVT1 +agomir-612

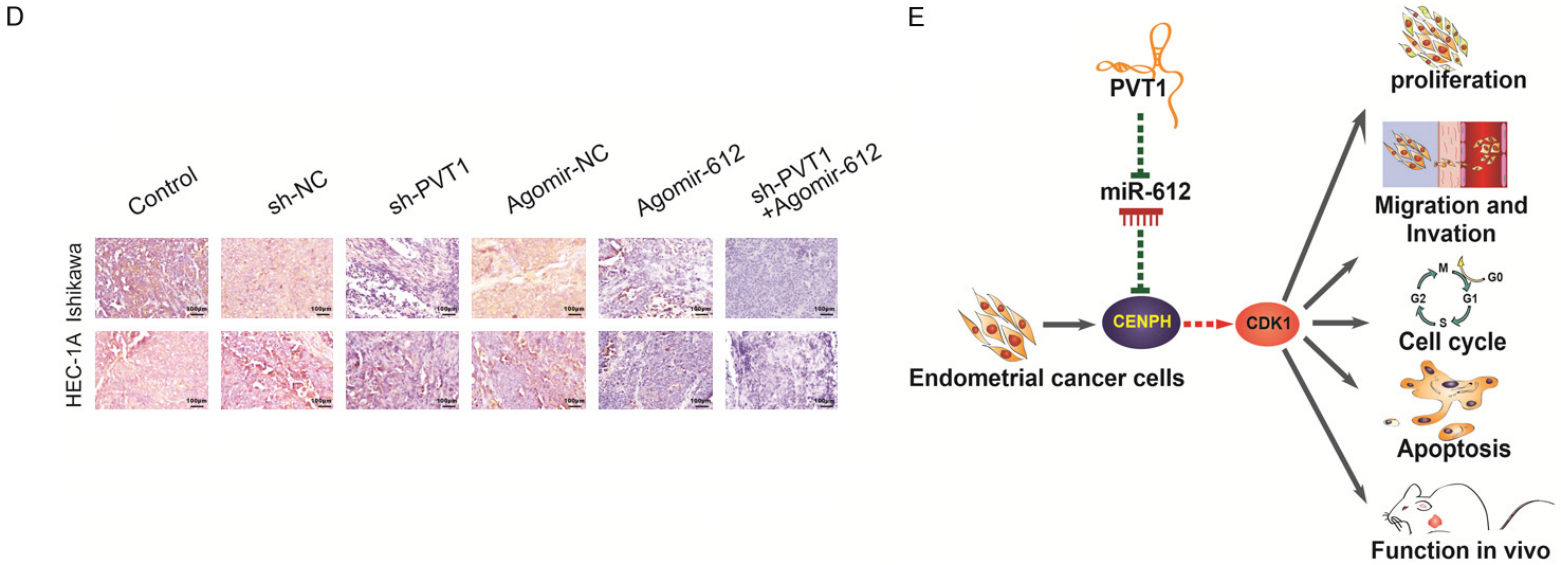

Figure 6. CDK1 connects PVT1/miR-612/CENP-H network and Akt/mTOR pathway, and tumour xenografts are constructed in vivo. A. Western blot analysis of the expression of CENP-H, CDK1, p-Akt, Akt, p-mTOR, mTOR in response to the altering of PVT1, miR-612 and CENP-H in Ishikawa and HEC-1A. Relative expression of β-actin is taken as an endogenous control. B. Nude mice harboring tumours are presented. C. The changes of tumour volume over time. D. Expression of CENP-H in mice tumour tissues are presented by IHC assays. Positive cells are stained brown. E. The working model suggests PVT1 acts as a miR-612 sponge to regulate CENP-H expression and influences biological behaviours of EC cells via interaction between CNP-H and CDK1. Data are presented as the mean ± SEM (n = 3 per group). $^{*}P < 0.05$, $^{**}P < 0.01$, $^{***}P < 0.001$ vs control group.

ducer and activator of transcription 3 (phospho-STAT3) by protecting it from poly-ubiquitination and proteasome-dependent degradation. As a result, the STAT3 signaling pathway was activated and tumour angiogenesis was promoted. Nevertheless, the effect of lncRNA PVT1 is not limited to a single pathway and the underlying mechanisms remain largely unknown. Therefore, we used the generally acknowledged TCGA database to conduct a PVT1-centered co-expression network to uncover the unknown interactions between PVT1 and other lncRNAs, miRNAs and mRNAs. The bioinformatics analysis could shed some light on the understanding of PVT1-related disease progression and help other scholars to discuss the underlying mechanisms of PVT1 in EC, as well as in other malignant diseases. We also conducted another analysis on high-stage EC to identify which interaction might lead to the malignant progression. The network suggested that PVT1 might contribute to the aggressive progression of EC via interaction with miR-612, miR-195, or miR-424. In the present study, we completed in-depth study of miR-612 in EC.

ISH and qRT-PCR analyses showed a low copy number of miR-612 in 57 EC tissues compared to 20 normal tissues, and the number continuously declined with increasing clinical stage. These observations were consistent with the previously reported tumour suppressor role of miR-612 in some other cancers. For example, miR-612 repressed bladder cancer by targeting malic enzyme 1 expression [20]. It also regulated ovarian cancer malignancy via the lncRNA LUCAT/miR-612/HOXA13 axis [21]. However, the mechanism of miR-612 in EC progression is still unknown. In our study, cells with downregulated miR-612 showed a strong increase in tumour cell proliferation, migration, and invasion. Furthermore, more cells were found at G2-M phase, and less apoptosis was observed. By contrast, overexpression of miR-612 lessened the malignant behaviour of EC cells.

To determine whether the anti-tumour effects of PVT1 downregulation are mediated by miR-612, we first conducted PCR tests and revealed the negative association between miR-612 and PVT1 expression. Then rescue experiments were conducted by studying the biological behaviour of the cell lines with downregulation of PVT1 and miR-612. The cells with PVT1(-)+miR-612(-) demonstrated less of an inhibition on tumour cell proliferation, migration, and invasion, and more apoptosis when compared to cells with downregulated PVT1 only. These findings demonstrate that an essential PVT1-miR-612 axis contributes to EC progression. Moreover, *in vivo* studies demonstrated that PVT1 knockdown, together with upregulation of miR-612, exerted the strongest anti-tumour effects in nude mice.

To determine the functional target of miR-612, we referred to three additional bioinformatics databases (TargetScan7, miRDB, RNA22v2.0), and all results suggested a centromere protein, CENP-H, as the functional target. CENP-H localizes at centromeres in the chromosome and works as part of the 16-subunit Constitutive Centromere-Associated Network (CCAN), which mediates the action of the centromere and the outer kinetochore throughout the cell cycle [22]. During cell division, centromeres are attached by spindle microtubules and then proceed through a series of centromere-kinetochore interactions. The components of CCAN play a pivotal role in these processes, but they are interacting with complex protein-protein networks which remain incompletely understood. Based on the existing literature, at beginning, the histone variant CENP-A replaces H3 at centromeres nucleosomes [23]. CENP-C recognizes CENP-A in conjunction with centromeric chromatin initiates the rest CCAN assembly [24]. CENP-N could also directly bind to CENP-A and keep maintenance of centromeric chromatin [25]. It is reported that CENP-C comes into effects via direct interactions with CENP-N and CENP-H/I/K/M, but meanwhile these interactions could reciprocally stabilize CENP-C itself [26]. CENP-H, together with CENP-I and CENP-K, forms as a core ternary of CCAN. This complex is essential for kinetochore integrity and loss of any component will compromise chromosome congression [27]. The C-terminal half of CENP-I binds to CENP-M. The CENP-H/I/K/M complex is required for recruiting or retaining CENP-T/W and maintains stable association between CENP-T/W and kinetochores [28]. CENP-T/W complex combines with CENP-S/X complex and forms a heterotetramer which preferentially binds to DNA fragments and induces positive DNA supercoils. The heterotetramer provides a crucial platform for the assembly of the centromere chromatin struc-

ture [29]. It has been reported that abnormal expression or location of CENP-H could lead to the disorders of cell division and chromosomal abnormalities, which are typical hallmarks of cancer. Wu [30] showed with transcriptome sequencing that the expression of CENP-H was remarkably increased in renal cell carcinoma. Lu [31] found that CENP-H was upregulated in hepatocellular carcinoma and closely related to tumour size, clinical stage, and histological grade. However, none of these studies have discussed whether CENP-H dysregulation is associated with certain miRNAs.

For the first time, we used dual-luciferase gene reporter assay to validate the binding site of miR-612 and the 3'-UTR of CENP-H. We investigated the expression of CENP-H in our specimens, and found CENP-H expression was markedly upregulated in EC tissues, especially in higher stages of disease. Our findings also suggested that CENP-H was associated with the survival time of EC patients and could serve as a novel diagnostic and prognostic indicator. Furthermore, we performed a series of assays to demonstrate the oncogenic role of CENP-H in EC. These assays showed that CENP-H promoted cell proliferation, migration, invasion, and inhibited cell apoptosis. Additionally, we showed that overexpression of CENP-H dampened the anti-tumour effects of miR-612. Together, these findings suggest that the expression of CENP-H could be a functional target of miR-612.

CENP-H expression has been previously reported to be associated with the Akt/mTOR pathway in colorectal cancer [32], but the relationship between CENP-H and Akt has not been discussed in EC. With the help of a bioinformatics database, we found that CDK1 may act as a medium between CENP-H and Akt. CDK1 belongs to the Ser/Thr protein kinase family, and serves as a catalytic subunit of a highly conserved protein kinase complex called M-phase promoting factor. Both CENP-H and CDK1 are believed to take part in the regulation of the cell cycle from G2 to M phase. In the late G2 phase, CDK1 becomes activated and forms the CDK1-cyclin B complex. This complex further phosphorylates many substrate proteins, including histone H1, lamins, and nucleolin, to promote the transition of cells from G2 to M phase [33]. Moreover, CDK1 has been reported to co-immunoprecipitation with phosphoinositide-dependent kinase 1 (PDK1) and participate in the kinase cascade mode of the CDK1-PDK1-Akt signaling pathway [16].

Importantly, CDK1 has been identified as an essential gene for tumour initiation and progression in different types of carcinomas. Qian [34] reported that CDK1 played an oncogenic role in breast cancer and could be regulated by KIAA1429 in an m6A-independent manner. Jin [35] demonstrated that CDK1 was highly expressed in hepatocellular carcinoma and that silencing of CDK1 promoted cell apoptosis, inhibited cell invasion, and regulated the cell cycle. Similar findings have been reported in EC, but the underlying mechanism of CDK1 has not been illustrated [36]. We conducted western blots and found that the expression of CDK1 was consistent with the changes of CENP-H expression, and that knockdown of CDK1 rescued the Akt/mTOR signaling pathway after si-CENP-H inhibition. According to the existing studies, we speculate that CENP-H complex might contribute to mitotic kinetochore localization of CENP-C and CENP-T, whose functions rely on the participant of CDK1. They could provide phosphorylation sites for CDK1 and recruit CDK1 in some way [37, 38]. Therefore, CDK1 might function as a bridge to connect the PVT1/miR-612/CENP-H ceRNA network and the Akt/mTOR signaling pathway.

Conclusion

In summary, the present study was the first to outline the PVT1-centered ceRNA network and suggested that the PVT1/miR-612/CENP-H/CDK1 axis might lead to the progression of advanced EC, as schematically presented in **Figure 6E**. We demonstrated that PVT1 acted as a sponge to capture miR-612, thereby regulating the oncogenic ability of CENP-H. Further studies on the correlation between CENP-H and clinicopathological factors suggests that CENP-H may serve as a novel diagnostic and prognostic indicator of EC. We also demonstrated that the functions of the PVT1/miR-612/CENP-H ceRNA network were mediated by the interaction between CENP-H and CDK1 towards the Akt/mTOR signaling pathway. Moreover, *in vivo* studies demonstrated that knockdown of PVT1 together with upregulation of miR-612

exerted the strongest anti-tumour effects in nude mice. Thus, the PVT1/miR-612/CENP-H/CDK1 axis could serve as a promising target for the potential treatment of advanced EC.

Acknowledgements

We are grateful for the financial support from the National Natural Science Foundation of China, University Innovation Team of Liaoning Province, "Major Special Construction Plan" for Discipline Construction of China Medical University, Liaoning Revitalization Talents Program, Special professor of Liaoning Province and Outstanding Scientific Fund of Shengjing Hospital. This work was supported by the National Natural Science Foundation of China (No. 81872123) and University Innovation Team of Liaoning Province (2018-479) for data collection, "Major Special Construction Plan" for Discipline Construction of China Medical University (No. 3110118029) and Liaoning Revitalization Talents Program (XLYC1902003) for data analysis, Special professor of Liaoning Province and Outstanding Scientific Fund of Shengjing Hospital (No. 201601) for writing. This study is approved by the Institutional Review Committee of the Ethics Committee of Shengjing Hospital of China Medical University (No. 2017PS292K) and it conforms to the provisions of the Declaration of Helsinki.

Disclosure of conflict of interest

None.

Abbreviations

PVT1, plasmacytoma variant translocation 1; EC, endometrial cancer; ceRNA, competing endogenous RNA; UCEC, Uterine Corpus Endometrial Carcinoma; TCGA, The Cancer Genome Atlas; lncRNA, long noncoding RNA; FIGO, International Federation of Gynecology and Obstetrics; CENP-H, Centromere protein-H; CDK1, cyclin dependent kinase 1; HEK, human embryonic kidney; DMEM, Dulbecco's Modified Eagle Medium; GAPDH, glyceraldehyde phosphate dehydrogenase; IHC, Immunohistochemistry; ISH, *in situ* hybridization; ANOVA, one-way analysis of variance; CCK-8, Cell counting kit-8; EdU, 5-Ethynyl-2'deoxyuridine; ROC, Receiver operating characteristic curves; AUC, area under curve; MDM2, mouse double minute 2; phospho-STAT3, phosphorylated signal transducer and activator of transcription 3; CCAN, Constitutive Centromere-Associated Network; PDK1, phosphoinositide-dependent kinase 1.

Address correspondence to: Xiaoxin Ma, Department of Obstetrics and Gynecology, Shengjing Hospital of China Medical University, No. 36 Sanhao Street, Shenyang 110004, People's Republic of China. Tel: +86-18904001666; E-mail: maxiaoxin666@aliyun.com

References

[1] Siegel RL, Miller KD and Jemal A. Cancer statistics, 2018. CA Cancer J Clin 2018; 68: 7-30.

[2] Dong P, Xiong Y, Yue J, J B Hanley S, Kobayashi N, Todo Y and Watari H. Exploring lncRNA-mediated regulatory networks in endometrial cancer cells and the tumor microenvironment: advances and challenges. Cancers (Basel) 2019; 11: 234.

[3] Arend RC, Jones BA, Martinez A and Goodfellow P. Endometrial cancer: molecular markers and management of advanced stage disease. Gynecol Oncol 2018; 150: 569-580.

[4] Nie Y, Zhou L, Wang H, Chen N, Jia L, Wang C, Wang Y, Chen J, Wen X, Niu C, Li H, Guo R, Zhang S, Cui J, Hoffman AR, Hu JF and Li W. Profiling the epigenetic interplay of lncRNA RUNXOR and oncogenic RUNX1 in breast cancer cells by gene in situ cis-activation. Am J Cancer Res 2019; 9: 1635-1649.

[5] Li T, Yang XD, Ye CX, Shen ZL, Yang Y, Wang B, Guo P, Gao ZD, Ye YJ, Jiang KW and Wang S. Long noncoding RNA HIT000218960 promotes papillary thyroid cancer oncogenesis and tumor progression by upregulating the expression of high mobility group AT-hook 2 (HMGA2) gene. Cell Cycle 2017; 16: 224-231.

[6] Cai R, Tang G, Zhang Q, Yong W, Zhang W, Xiao J, Wei C, He C, Yang G and Pang W. A novel lncRNA, named lnc-ORA, is identified by RNA-seq analysis, and its knockdown inhibits adipogenesis by regulating the PI3K/AKT/mTOR signaling pathway. Cells 2019; 8: 477.

[7] Huang Z, Du G, Huang X, Han L, Han X, Xu B, Zhang Y, Yu M, Qin Y, Xia Y, Wang X and Lu C. The enhancer RNA lnc-SLC4A1-1 epigenetically regulates unexplained recurrent pregnancy loss (URPL) by activating CXCL8 and NF-kB pathway. EBioMedicine 2018; 38: 162-170.

[8] Chen J, Yu Y, Li H, Hu Q, Chen X, He Y, Xue C, Ren F, Ren Z, Li J, Liu L, Duan Z, Cui G and Sun R. Long non-coding RNA PVT1 promotes tumor progression by regulating the miR-143/HK2 axis in gallbladder cancer. Mol Cancer 2019; 18: 33.

[9] Xu Y, Li Y, Jin J, Han G, Sun C, Pizzi MP, Huo L, Scott A, Wang Y, Ma L, Lee JH, Bhutani MS, Weston B, Vellano C, Yang L, Lin C, Kim Y, MacLeod AR, Wang L, Wang Z, Song S and Ajani JA. LncRNA PVT1 up-regulation is a poor prognosticator and serves as a therapeutic target in esophageal adenocarcinoma. Mol Cancer 2019; 18: 141.

[10] Tang J, Li Y, Sang Y, Yu B, Lv D, Zhang W and Feng H. LncRNA PVT1 regulates triple-negative breast cancer through KLF5/beta-catenin signaling. Oncogene 2018; 37: 4723-4734.

[11] Zhao J, Du P, Cui P, Qin Y, Hu C, Wu J, Zhou Z, Zhang W, Qin L and Huang G. LncRNA PVT1 promotes angiogenesis via activating the STAT3/VEGFA axis in gastric cancer. Oncogene 2018; 37: 4094-4109.

[12] Chai J, Guo D, Ma W, Han D, Dong W, Guo H and Zhang Y. A feedback loop consisting of RUNX2/LncRNA-PVT1/miR-455 is involved in the progression of colorectal cancer. Am J Cancer Res 2018; 8: 538-550.

[13] Kong F, Ma J, Yang H, Yang D, Wang C and Ma X. Long non-coding RNA PVT1 promotes malignancy in human endometrial carcinoma cells through negative regulation of miR-195-5p. Biochim Biophys Acta Mol Cell Res 2018; S0167-4889(18)30169-1.

[14] Xing TR, Chen P, Wu JM, Gao LL, Yang W, Cheng Y and Tong LB. UPF1 participates in the progression of endometrial cancer by inhibiting the expression of lncRNA PVT1. Onco Targets Ther 2020; 13: 2103-2114.

[15] Wang W, Zhou R, Wu Y, Liu Y, Su W, Xiong W and Zeng Z. PVT1 promotes cancer progression via microRNAs. Front Oncol 2019; 9: 609.

[16] Wang XQ, Lo CM, Chen L, Ngan ES, Xu A and Poon RY. CDK1-PDK1-PI3K/Akt signaling pathway regulates embryonic and induced pluripotency. Cell Death Differ 2017; 24: 38-48.

[17] Remmerie M and Janssens V. Targeted therapies in type II endometrial cancers: too little, but not too late. Int J Mol Sci 2018; 19: 2380.

[18] Wu S, Chen H, Han N, Zhang C and Yan H. Long noncoding RNA PVT1 silencing prevents the development of uveal melanoma by impairing microRNA-17-3p-dependent MDM2 upregulation. Invest Ophthalmol Vis Sci 2019; 60: 4904-4914.

[19] Shen SN, Li K, Liu Y, Yang CL, He CY and Wang HR. Down-regulation of long noncoding RNA PVT1 inhibits esophageal carcinoma cell migration and invasion and promotes cell apoptosis via microRNA-145-mediated inhibition of FSCN1. Mol Oncol 2019; 13: 2554-2573.

[20] Liu M, Chen Y, Huang B, Mao S, Cai K, Wang L and Yao X. Tumor-suppressing effects of microRNA-612 in bladder cancer cells by targeting malic enzyme 1 expression. Int J Oncol 2018; 52: 1923-1933.

[21] Yu H, Xu Y, Zhang D and Liu G. Long noncoding RNA LUCAT1 promotes malignancy of ovarian cancer through regulation of miR-612/HOXA13 pathway. Biochem Biophys Res Commun 2018; 503: 2095-2100.

[22] Hoischen C, Yavas S, Wohland T and Diekmann S. CENP-C/H/I/K/M/T/W/N/L and hMis12 but not CENP-S/X participate in complex formation in the nucleoplasm of living human interphase cells outside centromeres. PLoS One 2018; 13: e0192572.

[23] Black BE, Brock MA, Bedard S, Woods VL Jr and Cleveland DW. An epigenetic mark generated by the incorporation of CENP-A into centromeric nucleosomes. Proc Natl Acad Sci U S A 2007; 104: 5008-5013.

[24] Carroll CW, Milks KJ and Straight AF. Dual recognition of CENP-A nucleosomes is required for centromere assembly. J Cell Biol 2010; 189: 1143-1155.

[25] Carroll CW, Silva MC, Godek KM, Jansen LE and Straight AF. Centromere assembly requires the direct recognition of CENP-A nucleosomes by CENP-N. Nat Cell Biol 2009; 11: 896-902.

[26] McKinley KL, Sekulic N, Guo LY, Tsinman T, Black BE and Cheeseman IM. The CENP-L-N complex forms a critical node in an integrated meshwork of interactions at the centromere-kinetochore interface. Mol Cell 2015; 60: 886-898.

[27] Hu L, Huang H, Hei M, Yang Y, Li S, Liu Y, Dou Z, Wu M, Li J, Wang GZ, Yao X, Liu H, He X and Tian W. Structural analysis of fungal CENP-H/I/K homologs reveals a conserved assembly mechanism underlying proper chromosome alignment. Nucleic Acids Res 2019; 47: 468-479.

[28] Basilico F, Maffini S, Weir JR, Prumbaum D, Rojas AM, Zimniak T, De Antoni A, Jeganathan S, Voss B, van Gerwen S, Krenn V, Massimiliano L, Valencia A, Vetter IR, Herzog F, Raunser S, Pasqualato S and Musacchio A. The pseudo GTPase CENP-M drives human kinetochore assembly. Elife 2014; 3: e02978.

[29] Takeuchi K, Nishino T, Mayanagi K, Horikoshi N, Osakabe A, Tachiwana H, Hori T, Kurumizaka H and Fukagawa T. The centromeric nucleosome-like CENP-T-W-S-X complex induces positive supercoils into DNA. Nucleic Acids Res 2014; 42: 1644-1655.

[30] Wu X, Lin Y, Shi L, Huang Y, Lai C, Wang Y, Zhang M, Wang S, Heng B, Yu G, Du X, Fang L, Fu Y, Chen J, Guo Z, Su Z and Wu S. Upregulation of centromere protein H is associated with progression of renal cell carcinoma. J Mol Histol 2015; 46: 377-385.

[31] Lu G, Hou H, Lu X, Ke X, Wang X, Zhang D, Zhao Y, Zhang J, Ren M and He S. CENP-H regulates the cell growth of human hepatocellular carcinoma cells through the mitochondrial apoptotic pathway. Oncol Rep 2017; 37: 3484-3492.
[32] Wu W, Wu F, Wang Z, Di J, Yang J, Gao P, Jiang B and Su X. CENPH inhibits rapamycin sensitivity by regulating GOLPH3-dependent mTOR signaling pathway in colorectal cancer. J Cancer 2017; 8: 2163-2172.
[33] Yan GJ, Yu F, Wang B, Zhou HJ, Ge QY, Su J, Hu YL, Sun HX and Ding LJ. MicroRNA miR-302 inhibits the tumorigenicity of endometrial cancer cells by suppression of Cyclin D1 and CDK1. Cancer Lett 2014; 345: 39-47.
[34] Qian JY, Gao J, Sun X, Cao MD, Shi L, Xia TS, Zhou WB, Wang S, Ding Q and Wei JF. KIAA1429 acts as an oncogenic factor in breast cancer by regulating CDK1 in an N6-methyladenosine-independent manner. Oncogene 2019; 38: 6123-6141.
[35] Jin J, Xu H, Li W, Xu X, Liu H and Wei F. LINC00346 acts as a competing endogenous RNA regulating development of hepatocellular carcinoma via modulating CDK1/CCNB1 axis. Front Bioeng Biotechnol 2020; 8: 54.
[36] Li L, Qu YW and Li YP. Over-expression of miR-1271 inhibits endometrial cancer cells proliferation and induces cell apoptosis by targeting CDK1. Eur Rev Med Pharmacol Sci 2017; 21: 2816-2822.
[37] Watanabe R, Hara M, Okumura EI, Herve S, Fachinetti D, Ariyoshi M and Fukagawa T. CDK1-mediated CENP-C phosphorylation modulates CENP-A binding and mitotic kinetochore localization. J Cell Biol 2019; 218: 4042-4062.
[38] Huis In't Veld PJ, Jeganathan S, Petrovic A, Singh P, John J, Krenn V, Weissmann F, Bange T and Musacchio A. Molecular basis of outer kinetochore assembly on CENP-T. Elife 2016; 5: e21007.

Table S1. Association between CENPH and miR-612 expression with endometrial cancer patients clinicopathologic characteristics

Clinicopathological characters	Total (n = 57)	Low CENPH	High CENPH	P	Low miR-612	High miR-612	P
Age, y							
< 55	31	18	13	0.306	15	16	0.462
55-65	17	6	11		7	10	
> 65	9	4	5		6	3	
Stage							
I	16	14	2	< 0.001	15	1	< 0.001
II	16	12	4		7	9	
III	13	0	13		5	8	
IV	12	2	10		1	11	
Grade							
1	15	9	6	0.148	10	5	0.102
2	17	5	12		5	12	
3	25	14	11		13	12	
BMI, kg/m^2							
< 25	41	21	20	0.387	18	23	0.289
25-30	11	6	5		6	5	
> 30	5	1	4		4	1	
Lymphovascular space invasion							
Absent	6	1	5	0.093	25	28	0.283
Present	51	27	24		3	1	
Histopathological subtype							
Endometrioid	43	20	23	0.786	22	21	0.379
Stromal sarcoma	3	1	2		0	3	
Serous	2	1	1		1	1	
Mixed	4	3	1		3	1	
Carcinosarcoma	5	3	2		2	3	

Table S2. Primer sequences for qRT-PCR

Name	Sequence
PVT1	F: GCTGTGGCTGAATGCCTCAT R: TTCACCAGGAAGAGTCGGGG
miR-612	F: GGGCAGGGCTTCTGAGC
CENPH	F: CAGCCCCAGATGCAAGACG R: GCCTGAGGAGCAGGGTCAT
CDK1	F: TTTTCAGAGCTTTGGGCACT R: CCATTTTGCCAGAAATTCGT
GAPDH	F: GCACCGTCAAGGCTGAGAAC R: TGGTGAAGACGCCAGTGGA
U6	F: CGGGTTTGTTTTGCATTTCT R: AGTCCCAGCATGAACAGCTT

Table S3. The lentivirus, siRNA cloned and agomir and antagomir sequences

Name	Sequence
LV-NC	5'-TTCTCCGAACGTGTCACGT-3'
LV-PVT1-RNAi (47488-1)	5'-GCAGCTTATTATAGACTTA-3'
Agomir-NC	5'-UUCUCCGAACGUGUCACGUTT-3' Antisense: 5'-ACGUGACACGUUCGGAGAATT-3'
hsa-miR-612 agomir	GCUGGGCAGGGCUUCUGAGCUCCUU Antisense: 5'-GGAGCUCAGAAGCCCUGCCCAGCUU-3'
Antagomir-NC	5'-UUGUACUACACAAAAGUACUG-3'
hsa-miR-612 antagomir	AAGGAGCTCAGAAGCCCTGCCCAGC
Si-NC	5'-UUCUCCGAACGUGUCACGUTT-3' Antisense: 5'-ACGUGACACGUUCGGAGAATT-3'
CENPH-homo-484	5'-GCAGGAAUCUUGGGAUUUATT-3' Antisense: 5'-UAAAUCCCAAGAUUCCUGCTT-3'
CENPH-homo-754	5'-GGAAAUUGUUCUGCAGCUUTT-3' Antisense: 5'-AAGCUGCAGAACAAUUUCCTT-3'
CENPH-homo-356	5'-GCAUUAGACAGGAUGAGACTT-3' Antisense: 5'-GUCUCAUCCUGUCUAAUGCTT-3'
CDK1-homo-269	5'-GGGGUUCCUAGUACUGCAATT-3' Antisense: 5'-UUGCAGUACUAGGAACCCCTT-3'
CDK1-homo-980	5'-GGCACUGAAUCAUCCAUAUTT-3' Antisense: 5'-AUAUGGAUGAUUCAGUGCCTT-3'
CDK1-homo-843	5'-CAGGACUAUAAGAAUACAUTT-3' Antisense: 5'-AUGUAUUCUUAUAGUCCUGTT-3'

Table S4. Primary antibodies used for the detection of protein expression

Name	Manufacturer	Dilution ratio: (*Western blotting, Immunohistochemistry*)
CENPH	Abcam, Cambridge, UK (ab224159)	1:200; 1:500
CDK1	Santa Cruz Biothechnology, CA (SC-54)	1:800
AKT	Proteintech, Hangzhou, China (60203-2-Ig)	1:4000
pAKT (S473)	Proteintech, Hangzhou, China (66444-1-Ig)	1:5000
mTOR	Proteintech, Hangzhou, China (20657-1-AP)	1:500
pmTOR (S2448)	Abcam, Cambridge, UK (ab84400)	1:1000
β-actin	Abcam, Cambridge, UK (ab8226)	1:1000

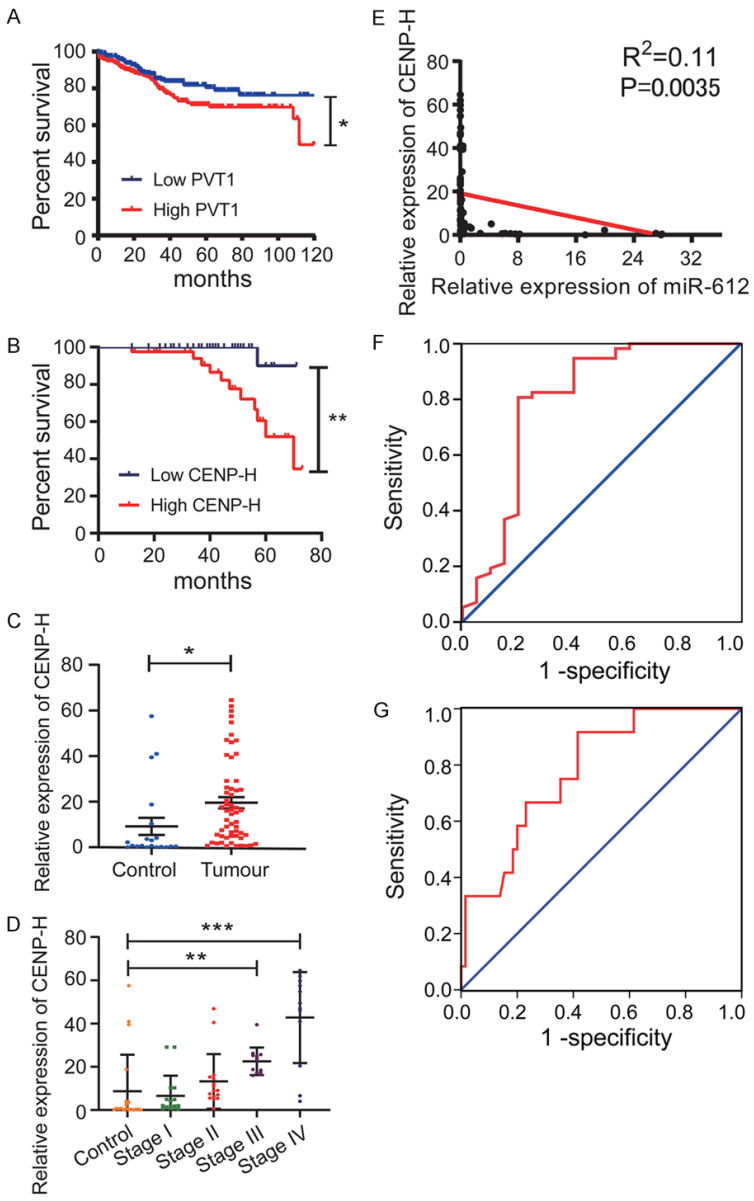

Figure S1. A. The association between PVT1 levels and EC patients survival. B. Relative CENP-H mRNA expression in EC tissues and normal tissues. C. Association between CENP-H mRNA expression and survival of EC patients. D. Relative CENP-H mRNA expression in different stages EC tissues and normal tissues. E. Pearson's test to analyze the correlation between miR-612 and CENP-H. F. Diagnostic Receiver operating characteristic curve (ROC) is performed to evaluate the diagnostic value of CENP-H. The area under curve (AUC) is 0.796 (95% CI = 0.655-0.936, P < 0.001). G. Prognostic ROC is performed to evaluate the prognostic value of CENP-H. The AUC is 0.783 (95% CI = 0.657-0.908, P = 0.002). *P < 0.05, **P < 0.01, ***P < 0.001 vs control group.

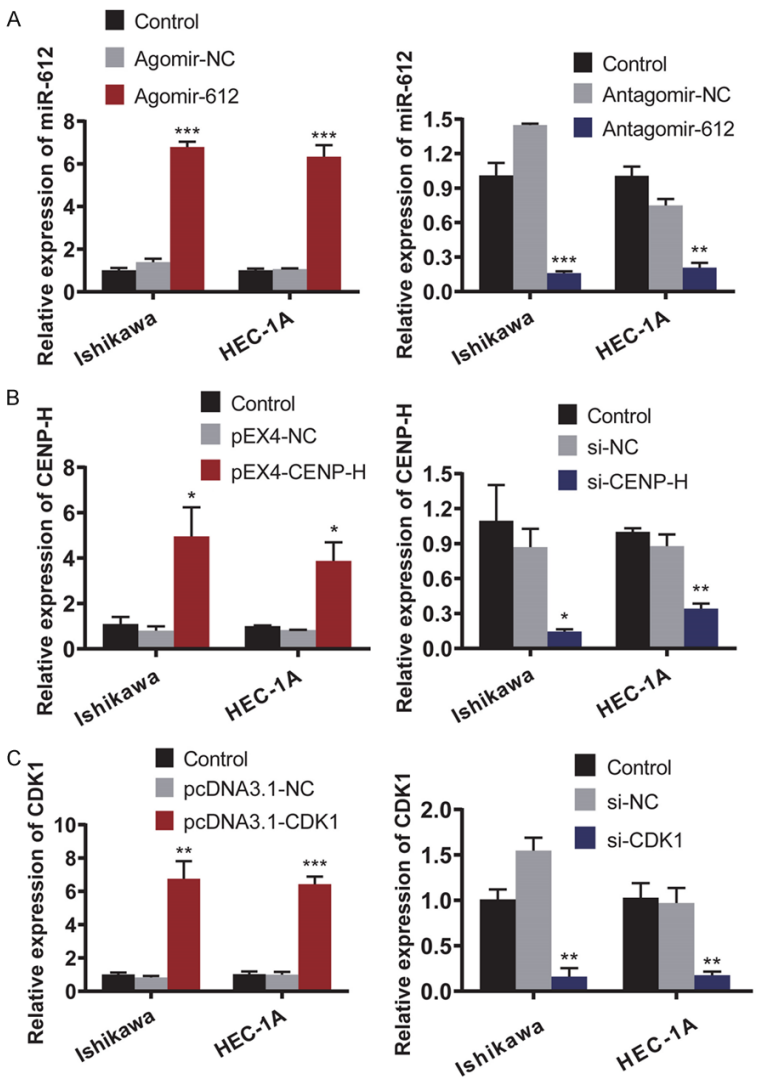

Figure S2. A. Transfection efficiency of miR-612 detected by qRT-PCR. B. Transfection efficiency of CENP-H detected by qRT-PCR. C. Transfection efficiency of CDK1 detected by qRT-PCR. Data are presented as the mean ± SEM (n = 3 per group). $^{*}P < 0.05$, $^{**}P < 0.01$, $^{***}P < 0.001$ vs NC group.

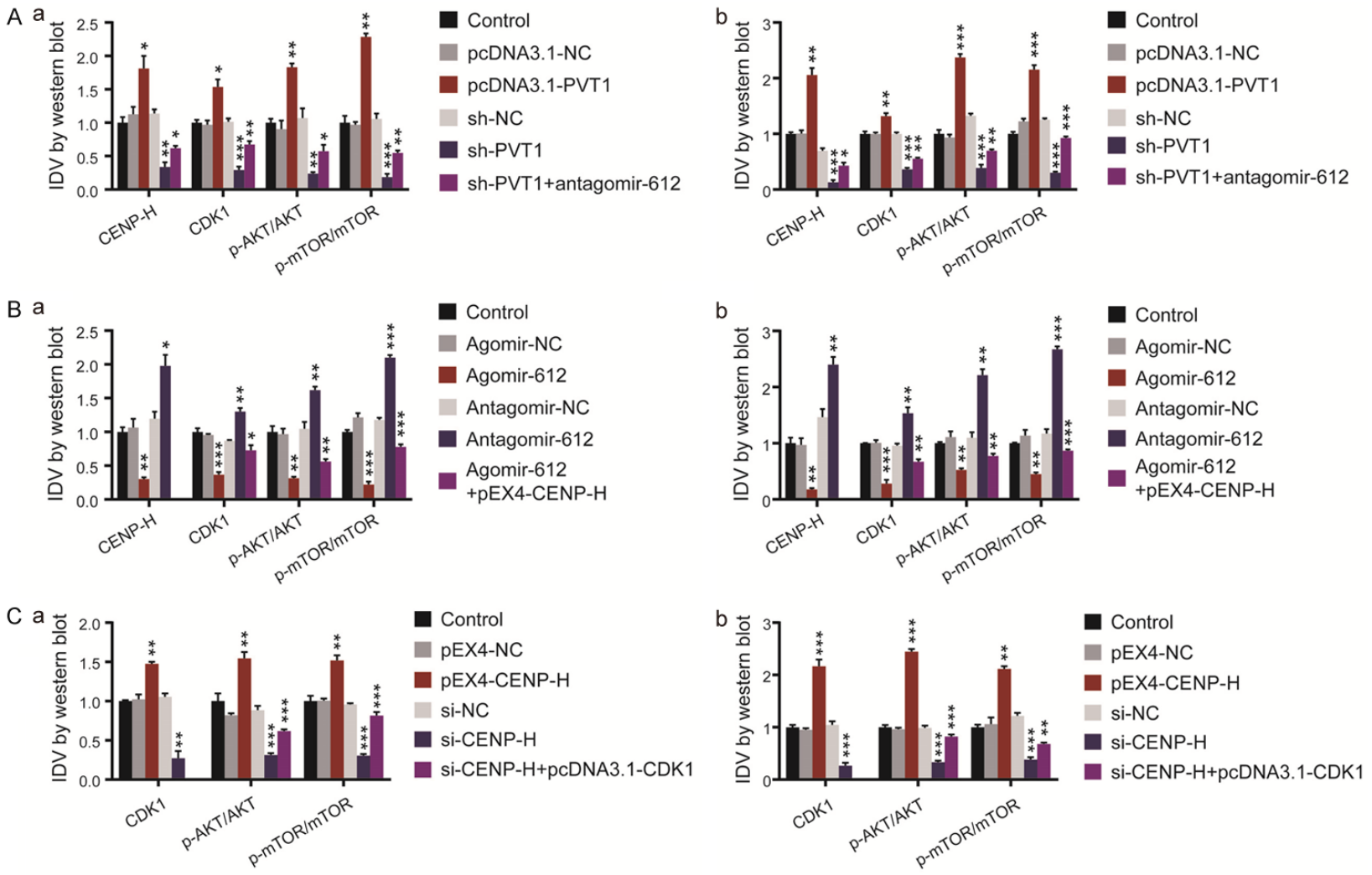

Figure S3. A. Western blot analysis of CENP-H/CDK1 and Akt/mTOR pathway regulated by PVT1 and miR-612. B. Western blot analysis of CENP-H/CDK1 and Akt/mTOR pathway regulated by miR-612 and CENP-H. C. Western blot analysis of CDK1 and Akt/mTOR pathway regulated by CENP-H and CDK1. Bar graphs display mean ± SD (n = 3 per group). $^{*}P < 0.05$, $^{**}P < 0.01$, $^{***}P < 0.001$ vs NC group.